JOC Article
pubs.acs.org/joc

Synthesis of and Evidence for Electronic Communication within Heteromultimetallic Tetrakis(NCN-pincer metal)−(Metallo)porphyrin Hybrids

Bart M. J. M. Suijkerbuijk,[†] Duncan M. Tooke,[‡] Martin Lutz,[‡] Anthony L. Spek,[‡] Leonardus W. Jenneskens,[†] Gerard van Koten,[†] and Robertus J. M. Klein Gebbink*[,†]

[†]*Organic Chemistry & Catalysis, Debye Institute for Nanomaterials Science, Faculty of Science, Utrecht University, Padualaan 8, 3584 CH Utrecht, The Netherlands, and* [‡]*Crystal and Structural Chemistry, Bijvoet Center for Biomolecular Research, Faculty of Science, Utrecht University, Padualaan 8, 3584 CH Utrecht, The Netherlands*

r.j.m.kleingebbink@uu.nl

Received November 19, 2009

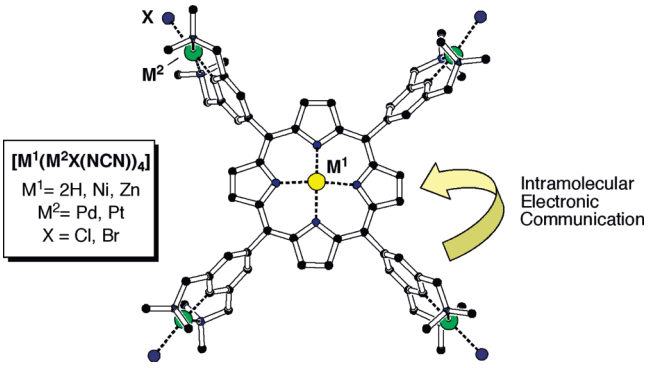

Several heteromultimetallic pincer−porphyrin hybrids have been prepared in excellent yields by stepwise metalation of a general precursor, [**2H**(**Br**(**NCN**))$_4$], which was designed in such a way so as to guarantee selectivity for either the porphyrin or pincer sites during the metalation steps. First, a metal was introduced in the porphyrin cavity using a metal(II) salt, followed by metalation of the pincer units through oxidative addition to an appropriate metal(0) complex. The resulting multimetallic complexes show an appreciable amount of intramolecular communication between the *meso*-pincer metal groups and the central metalloporphyrin component. This was manifested in changes of the optical and ligand-binding properties of the metalloporphyrin part upon reactions at the peripheral pincer sites.

Introduction

In general, the electron density on the metal center of transition metal complexes is of great importance for their properties. It determines several key features of the complex, such as the rate of ligand exchange, its optical properties, and redox characteristics.[1] The ability to fine-tune the electron density on the metal center of a complex is therefore of great value as a tool for the modulation of its coordination and physical properties, and therefore of, e.g., its catalytic activity. One of the most straightforward ways to effectuate this is to alter the ligands that coordinate to the metal ion. Within a certain group of ligands, further fine-tuning may be accomplished by attaching electron-withdrawing or -donating,[2−8] or even redox-active substituents[9−11] to the ligand. The success of this approach hinges on the extent

*To whom correspondence should be addressed. Phone: +31-30-2531889. Fax: +31-30-2523615.

(1) Cotton, F. A.; Wilkinson, G. *Advanced Inorganic Chemistry*, 5th ed.; John Wiley & Sons: New York, 1988.

(2) Abashkin, Y. G.; Collins, J. R.; Burt, S. K. *Inorg. Chem.* **2001**, *40*, 4040–4048.

(3) Benaglia, M.; Benincori, T.; Mussini, P.; Pilati, T.; Rizzo, S.; Sannicolò, F. *J. Org. Chem.* **2005**, *70*, 7488–7495.

(4) Berkessel, A.; Kaiser, P.; Lex, J. *Chem.—Eur. J.* **2003**, *9*, 4746–4756.

(5) Flanagan, S. P.; Guiry, P. J. *J. Organomet. Chem.* **2006**, *691*, 2125–2154.

(6) Gregson, C. K. A.; Blackmore, I. J.; Gibson, V. C.; Long, N. J.; Marshall, E. L.; White, A. J. P. *Dalton Trans.* **2006**, 3134–3140.

(7) Hu, A.; Ngo, H. L.; Lin, W. *Angew. Chem., Int. Ed.* **2004**, *43*, 2501–2504.

Published on Web 01/29/2010 DOI: 10.1021/jo902402g

CHART 1. General Formula of the Heteromultimetallic Pincer−Porphyrin Hybrid Complexes Presented Here

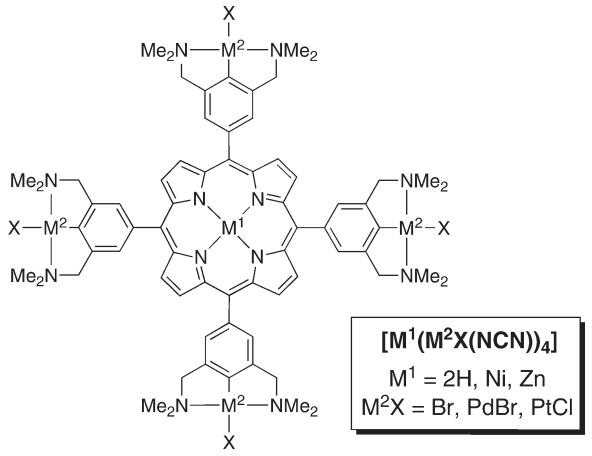

to which the electronic properties of the metal are coupled to those of its ligand(s). In most cases each member of a series of electronically modified ligands has to be synthesized independently, which may be very time-consuming. Ideally, one would like to be able to more readily change the electron density at the metal center. One strategy would be to covalently attach a modular substituent to, or merge it with, a metal complex. In this case, the electronic properties of the substituent should be easily, or maybe even in situ, tunable to bring about changes in the properties of the metal complex as a whole. By doing so, a series of electronically diverse metal complexes may be obtained readily from one common starting compound in, ideally, one step. This paper describes the exploration of this modular strategy by studying a series of hybrid complexes[12] that combine NCN-pincer-type organometallics with (metallo)porphyrins in a covalent manner (Chart 1).

For NCN-pincer-type organometallic complexes[13] (with the NCN-pincer being the monoanionic, potentially tridentate ligand $[2,6\text{-}(Me_2NCH_2)_2C_6H_3]^-$, Figure 1), the electron density on the ligated metal is known to be influenced strongly by the aryl-substituent at the para-position relative to the carbon-to-metal σ-bond. We have recently shown that the electron density on the chelated metal in para-substituted NCN-pincer Ni[14,15] and Pt[16,17] complexes [MX(NCN-Z)]

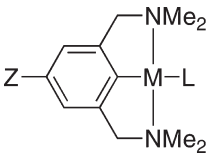

FIGURE 1. Schematic representation of para-substituted NCN-pincer ML complexes [ML(NCN-Z)]: Z = H_2N, HO, *t*-Bu, Me_3Si, H, I, HOOC, OHC, O_2N; M = Ni, Pd, Pt; L = Cl, Br, I, OH_2, Lewis base.

(MX = NiBr or PtCl) depends on the electron-donating or -withdrawing properties of the para-substituent Z, as indexed by its σ_p Hammett substituent constant. Furthermore, it has been demonstrated that the catalytic activity of several para-substituted NCN-pincer Pd aqua complexes in the double Michael addition reaction of ethyl α-cyano acetate to methyl vinyl ketone changes when the electronic properties of the para-substituent are varied.[18] In these cases, however, modularity of the tuning of the electron density on the metal center is precluded by the need for extensive synthetic chemistry to introduce each different para-substituent with its specific electronic properties onto the ligand.

Kim et al. synthesized a series of *meso*-mono- and -bis-(ferrocenyl)-substituted *β*-octakis(alkyl) metalloporphyrins and very elegantly showed that the (metallo)porphyrin unit can be used as a highly modular substituent to tune the electronic properties of the attached ferrocene groups (Figure 2, left).[19,20] It was found that a change of the metal in the porphyrin cavity was communicated to the *meso*-ferrocene units and consequently led to changes in their redox potentials. Those changes could be rationalized by taking the electronic properties of the (metallo)porphyrin into consideration. Arnold and co-workers synthesized (metallo)-porphyrins that act as monodentate ligands for palladium(II) and platinum(II) complexes (Figure 2, right).[21−28] They were able to introduce several metals inside and outside of the porphyrin ring and showed that ligand exchange at the peripheral palladium and platinum sites is possible, and that multidentate ligands could be introduced. Importantly, they showed that both metal centers influence each other.

In analogy to these examples, it was anticipated that a metalloporphyrin could be a highly modular pincer para-substituent. Not only do the electronic properties of

(8) Pillsbury, D. G.; Busch, D. H. *J. Am. Chem. Soc.* **1976**, *98*, 7836–7839.
(9) Allgeier, A. M.; Mirkin, C. A. *Angew. Chem., Int. Ed.* **1998**, *37*, 894–908.
(10) Gregson, C. K. A.; Gibson, V. C.; Long, N. J.; Marshall, E. L.; Oxford, P. J.; White, A. J. P. *J. Am. Chem. Soc.* **2006**, *128*, 7410–7411.
(11) Lorkovic, I. M.; Duff, R. R.; Wrighton, M. S. *J. Am. Chem. Soc.* **1995**, *117*, 3617–3618.
(12) Suijkerbuijk, B. M. J. M.; Klein Gebbink, R. J. M. *Angew. Chem., Int. Ed.* **2008**, *47*, 7396–7421.
(13) Albrecht, M.; van Koten, G. *Angew. Chem., Int. Ed.* **2001**, *40*, 3750–3781.
(14) van de Kuil, L. A.; Luitjes, H.; Grove, D. M.; Zwikker, J. W.; van der Linden, J. G. M.; Roelofsen, A. M.; Jenneskens, L. W.; Drenth, W.; van Koten, G. *Organometallics* **1994**, *13*, 468–477.
(15) van de Kuil, L. A.; Grove, D. M.; Gossage, R. A.; Zwikker, J. W.; Jenneskens, L. W.; Drenth, W.; van Koten, G. *Organometallics* **1997**, *16*, 4985–4994.
(16) Slagt, M. Q.; Rodríguez, G.; Grutters, M. M. P.; Klein Gebbink, R. J. M.; Klopper, W.; Jenneskens, L. W.; Lutz, M.; Spek, A. L.; van Koten, G. *Chem.—Eur. J.* **2004**, *10*, 1331–1344.
(17) Tromp, M.; van Bokhoven, J. A.; Slagt, M. Q.; Klein Gebbink, R. J. M.; van Koten, G.; Ramaker, D. E.; Koningsberger, D. C. *J. Am. Chem. Soc.* **2004**, *126*, 4090–4091.
(18) Dijkstra, H. P.; Slagt, M. Q.; McDonald, A.; Kruithof, C. A.; Kreiter, R.; Mills, A. M.; Lutz, M.; Spek, A. L.; Klopper, W.; van Klink, G. P. M.; van Koten, G. *Eur. J. Inorg. Chem.* **2003**, 830–838.
(19) Kim, J.; Rhee, S. W.; Na, Y. H.; Lee, K. P.; Do, Y.; Jeoung, S. C. *Bull. Korean Chem. Soc.* **2001**, *22*, 1316–1322.
(20) Rhee, S. W.; Na, Y. H.; Do, Y.; Kim, J. *Inorg. Chim. Acta* **2000**, *309*, 49–56.
(21) Arnold, D. P.; Healy, P. C.; Hodgson, M. J.; Williams, M. L. *J. Organomet. Chem.* **2000**, *607*, 41–50.
(22) Arnold, D. P.; Sakata, Y.; Sugiura, K.-I.; Worthington, E. I. *Chem. Commun.* **1998**, 2331–2332.
(23) Hartnell, R. D.; Arnold, D. P. *Organometallics* **2004**, *23*, 391–399.
(24) Hartnell, R. D.; Arnold, D. P. *Eur. J. Inorg. Chem.* **2004**, 1262–1269.
(25) Hartnell, R. D.; Edwards, A. J.; Arnold, D. P. *J. Porphyrins Phthalocyanines* **2002**, *6*, 695–707.
(26) Hodgson, M. J.; Borovkov, V. V.; Inoue, Y.; Arnold, D. P. *J. Organomet. Chem.* **2006**, *691*, 2162–2170.
(27) Hodgson, M. J.; Healy, P. C.; Williams, M. L.; Arnold, D. P. *J. Chem. Soc., Dalton Trans.* **2002**, 4497–4504.
(28) Kato, A.; Hartnell, R. D.; Yamashita, M.; Miyasaki, H.; Sugiura, K.-I.; Arnold, D. P. *J. Porphyrins Phthalocyanines* **2004**, *8*, 1222–1227.
(29) Dolphin, D. *The Porphyrins*; Academic Press, Inc.: New York, 1978.

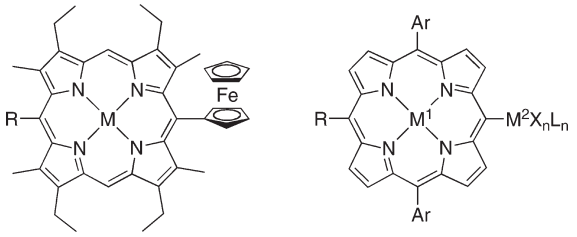

FIGURE 2. *meso*-Ferrocenyl (metallo)porphyrins prepared by Kim et al. (left; R = phenyl or ferrocenyl; M = 2H, MnCl, Ni, Zn) and *meso*-η^1-metalloporphyrins developed by Arnold and co-workers (right; R = H, phenyl, PdX_nL_n, PtX_nL_n; M^1 = 2H, MnCl, Co, Ni, Zn; $M^2X_nL_n$ = PdX_nL_n, PtX_nL_n).

metalloporphyrins strongly depend on the incorporated metal,[29−31] in addition most metals can be introduced in the porphyrin system in a single step with use of mild reaction conditions. Rather than having to go through elaborate syntheses to introduce each new para-substituent in the classical para-substituted metallopincer systems, a metal ion introduction step would suffice to change its electronic properties and consequently those of the pincer metal complex. The viability of this approach was shown recently by Osuka and co-workers.[32]

Conversely, the modulation of the electronic properties of (metallo)porphyrin systems, which can lead to variations in their electrochemical and photophysical properties, and coordination chemistry,[29,31] has also attracted considerable attention. The attachment of derivatized phenyl groups at the *meso*-position(s), for example, has been proven to be a powerful tool in this respect. The use of metal complexes for this purpose creates the possibility of, for example, redox coupling between the two moieties or electronic interaction in general.

Here, we present our efforts toward the development of a hybrid ligand system that will allow for the exploration of the concept of modular substituents in catalysis. A synthetic study toward *meso*-tetrakis(NCN-pincer M^2X)−porphyrin-(M^1) hybrids ([$\mathbf{M^1(M^2X(NCN))_4}$]: M^1 = 2H, Ni, Zn; M^2X = Br, PdBr, PtCl) of the type depicted in Chart 1, and, in particular, ways to address each coordination site, i.e., NCN-pincer ligand and porphyrin, independently and thus orthogonally are presented. We, furthermore, studied qualitatively the effect of alterations at one metal site on the properties of the second metal site in these hybrid systems.

Results

I. Synthesis. A successful protocol for the synthesis of the targeted heteromultimetallic molecules requires a building block consisting of a free-base porphyrin with NCN-pincer ligands attached to its four *meso*-positions. Selective metalation of either ligand site relies on the availability of orthogonal methods to address each moiety selectively and independently. Since porphyrins are often metalated using M(II) sources, we anticipated that metalation of the peripheral pincer ligands through oxidative addition of for instance an aryl bromide to an appropriate M(0) center would provide us with an orthogonal metalation protocol (see the Discussion section for a more in-depth discussion of this matter). To this end, we aimed at synthesizing porphyrin [**2H(Br(NCN))$_4$**], which has 3,5-bis[(dimethylamino)methyl]-4-bromophenyl groups at its *meso*-positions (Chart 1). To obtain [**2H(Br(NCN))$_4$**] we used a similar approach as during the synthesis of the previously described [**2H(H(NCN))$_4$**], in which an Adler-type cyclo-condensation of an appropriately functionalized benzaldehyde was used to form the porphyrin ring.[33] In addition, benzylic methoxide groups were used as masking groups for benzylic bromide functionalities, as the latter were expected to be too reactive to be carried throughout the whole synthetic route.

The functionalized benzaldehyde required for the Adler procedure, i.e., 3,5-bis(methoxymethyl)-4-bromobenzaldehyde (**4**, Scheme 1), was prepared from 3,5-bis(hydroxymethyl)-4-bromoiodobenzene (**1**), which itself was obtained from 3,5-dimethylaniline in six steps.[34] The direct preparation of 3,5-bis(methoxymethyl)-4-bromoiodobenzene (**3**) from **1** by treatment with NaH/MeI was hampered by partial reduction of the aryl bromide bond leading to an inseparable product mixture. Instead, 3,5-bis(chloromethyl)-4-bromoiodobenzene (**2**) was prepared in 93% yield by treatment of **1** with methane sulfonylchloride in triethylamine/THF (Scheme 1).[35] Subsequent nucleophilic substitution of the chloride groups with use of sodium methoxide in methanol proceeded readily to give **3** in 90% isolated yield. Lithiation of **3** at the iodo-position with *t*-BuLi (2 equiv) in THF at −100 °C and reaction of the resulting phenyl lithium species with DMF gave **4** in an optimized yield of 86%. During the synthesis of **4** it was noted that the selective lithiation of **3** at the iodo-position was impeded by a competing lithiation at the bromo-position. This was caused by the presence of the two hard benzylic oxygen donors, which can intramolecularly stabilize the 4-lithio species.[36] By performing the reaction at lower temperatures for shorter times, the formation of the thermodynamic 4-lithio intermediate could be successfully suppressed in favor of the kinetic 1-lithio intermediate.

The resulting bis(methoxymethyl)-4-bromobenzaldehyde (**4**) was used in an Adler-type condensation reaction[37] with pyrrole in refluxing propionic acid to give *meso*-tetrakis[3,5-bis(methoxymethyl)-4-bromophenyl]porphyrin (**5**) in 20% yield (Scheme 2). The procedures developed by Lindsey et al., which rely on the formation of a porphyrinogen, catalyzed by for example $BF_3 \cdot OEt_2$/NaCl or trifluoroacetic acid,[38] were also attempted for the synthesis of **5**. However, the former conditions led to cleavage of the benzylic ether

(30) Liao, M.-S.; Scheiner, S. *J. Chem. Phys.* **2002**, *117*, 205–219.
(31) Smith, K. M. *Porphyrins and Metalloporphyrins*; Elsevier Scientific Publishing Company: Amsterdam, The Netherlands, 1975.
(32) Yamaguchi, S.; Katoh, T.; Shinokubo, H.; Osuka, A. *J. Am. Chem. Soc.* **2007**, *129*, 6392–6393.
(33) Suijkerbuijk, B. M. J. M.; Lutz, M.; Spek, A. L.; van Koten, G.; Klein Gebbink, R. J. M. *Org. Lett.* **2004**, *6*, 3023−3026.
(34) Rodríguez, G.; Albrecht, M.; Schoenmaker, J.; Ford, A.; Lutz, M.; Spek, A. L.; van Koten, G. *J. Am. Chem. Soc.* **2002**, *124*, 5127–5138.
(35) Kruithof, C. A.; Casado, M. A.; Guillena, G.; Egmond, M. R.; van der Kerk, A.; Heck, A. J. R.; Klein Gebbink, R. J. M.; van Koten, G. *Chem.—Eur. J.* **2005**, *11*, 6869–6877.
(36) Jambor, R.; Dostál, L.; Císařová, I.; Ružička, A.; Holeček, J. *Inorg. Chim. Acta* **2005**, *358*, 2422–2426.
(37) Adler, A. D.; Longo, F. R.; Finarelli, J. D.; Goldmacher, J.; Assour, J.; Korsakoff, L. *J. Org. Chem.* **1967**, *32*, 476.
(38) Geier, G. R. III; Ciringh, Y.; Li, F.; Haynes, D. M.; Lindsey, J. S. *Org. Lett.* **2000**, *2*, 1745–1748.
(39) Dijkstra, H. P.; Meijer, M. D.; Patel, J.; Kreiter, R.; van Klink, G. P. M.; Lutz, M.; Spek, A. L.; Canty, A. J.; van Koten, G. *Organometallics* **2001**, *20*, 3159–3168.

SCHEME 1. Synthetic Route toward Functionalized Benzaldehyde 4

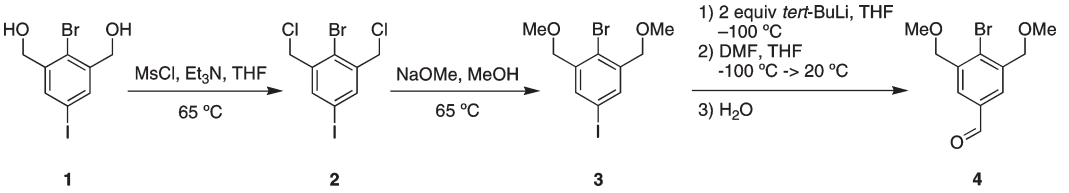

SCHEME 2. Synthetic Route toward [2H(Br(NCN))$_4$]

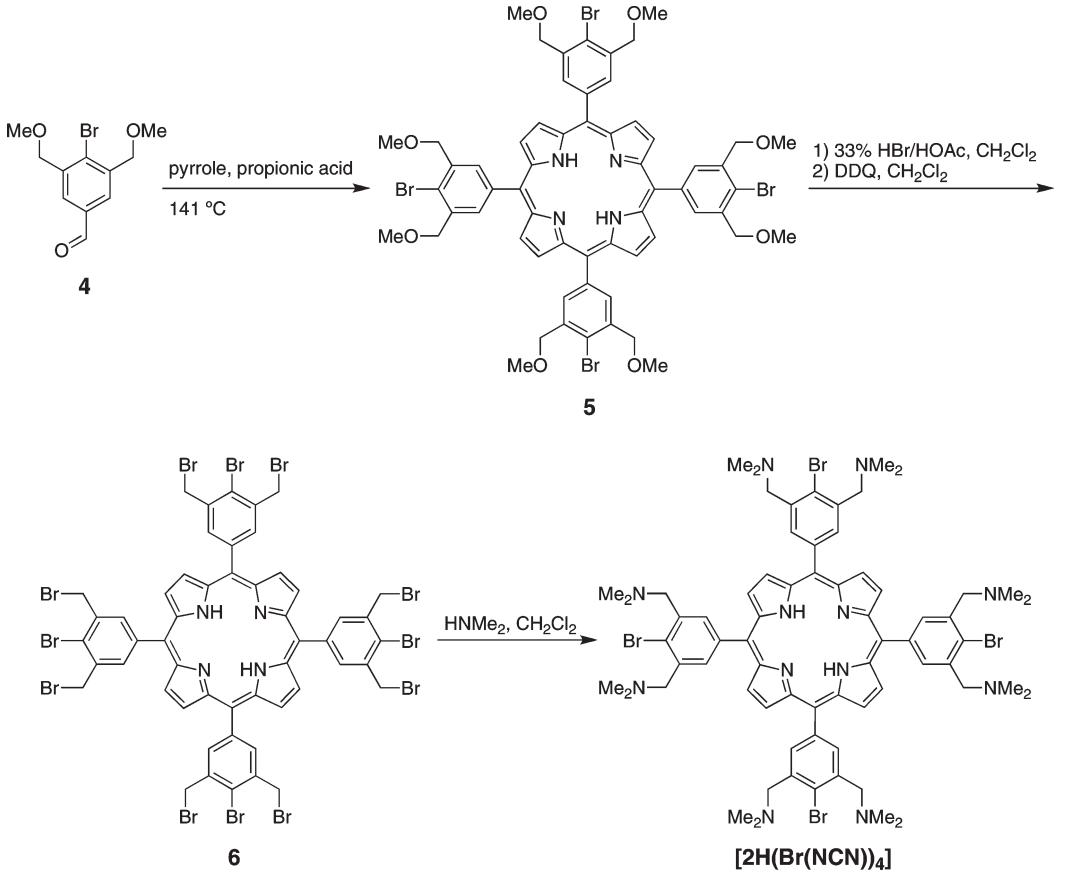

fragments (cf. Dijkstra et al.[39]), whereas the latter conditions led to difficulties during purification. Next, the methoxymethyl groups of **5** were converted into bromomethyl functionalities by using a fresh solution of HBr in acetic acid to give tetrakis[3,5-bis(bromomethyl)-4-bromophenyl]porphyrin (**6**) in 82% yield (Scheme 2).[33,40] During this step we noted that the use of Br_2-free HBr/HOAc is imperative, since traces of Br_2 impurities lead to partial β-bromination as evidenced by MALDI-TOF MS and ^{1}H NMR spectroscopy. Since the products of Adler-type porphyrin syntheses are invariably contaminated with the corresponding chlorines, crude **6** was treated with 2,3-dichloro-5,6-dicyanobenzoquinone (DDQ). This oxidation step was performed after the bromo-demethoxylation reaction because the separation of the polar polyether porphyrin **5** from DDQ and $DDQH_2$ proved to be difficult. Fortunately, the less polar nature of **6** allows for its straightforward isolation and purification by column chromatography on silica gel. The benzylic bromine atoms of **6** can be readily replaced through nucleophilic substitution as was shown earlier by us in the synthesis of a series of tetrapincer−porphyrin hybrids.[33] The ditopic ligand *meso*-tetrakis(3,5-bis[(dimethylamino)methyl]-4-bromophenyl)-porphyrin [**2H(Br(NCN))$_4$**] was isolated in 99% yield from the reaction of **6** with an excess of dimethylamine in CH_2Cl_2 (Scheme 2).

Because of the sensitivity of benzylic dimethylamino groups toward singlet oxygen,[41] this compound was stored and handled in the absence of molecular oxygen and light. The structural identity and product homogeneity of all compounds were confirmed by ^{1}H NMR and ^{13}C NMR spectroscopy, elemental analysis, mass spectrometry, and UV/vis spectroscopy. Porphyrin [**2H(Br(NCN))$_4$**] was subsequently subjected to several metalation procedures to selectively metalate the peripheral pincer groups and the central porphyrin core, to finally obtain the heteromultimetallic pincer−porphyrin hybrids [**M^1(M^{2}X(NCN))$_4$**].

(40) Jux, N. *Org. Lett.* **2000**, *2*, 2129–2132.

(41) Baciocchi, E.; Del Giacco, T.; Lapi, A. *Org. Lett.* **2004**, *6*, 4791–4794.

SCHEME 3. Synthetic Routes Leading to $[2H(M^2X(NCN))_4]$, $[M^1(Br(NCN))_4]$, and $[M^1(M^2X(NCN))_4]$

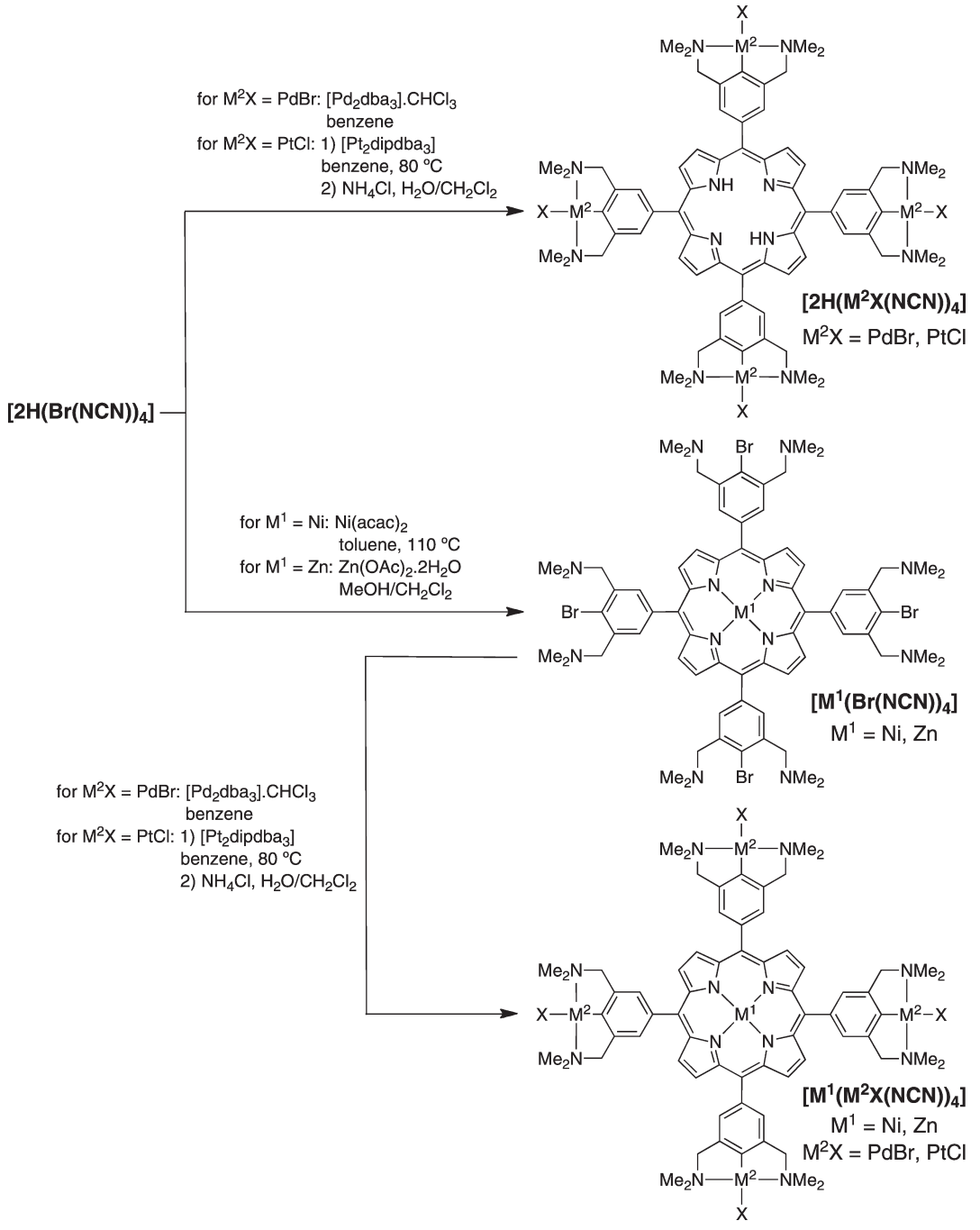

Selective Peripheral Metalation. In principle, the aryl bromide bonds of the peripheral NCN-pincer ligand groups of $[2H(Br(NCN))_4]$ can oxidatively add to suitable metal [M(0)] sources to give the peripherally metalated complexes $[2H(M^2X(NCN))_4]$. We chose to focus on the metals of the nickel triad, since the corresponding NCN-pincer metal complexes are applicable as catalysts, sensors, and as Lewis acids in materials chemistry.[14,16,18,42]

The peripheral platination of $[2H(Br(NCN))_4]$ was performed with $[Pt_2dipdba_3]$ (dipdba = 4,4′-diisopropylbenzylidene acetone),[43] which proved superior among several other platination reagents (vide infra), to give $[2H(PtX(NCN))_4]$ (X = halide) in 90% yield (Scheme 3). Benzene was used as a solvent for this reaction since the use of THF[44] gave rise to the formation of black impurities, which were inseparable from the product. $[2H(PtX(NCN))_4]$ is almost exclusively soluble in chlorinated solvents like CH_2Cl_2 and $CHCl_3$. Solubilization of $[2H(PtX(NCN))_4]$ in these solvents, however, is accompanied by fast halide exchange to give *meso*-tetrakis(NCN-pincer PtX)porphyrins in which

(42) Singleton, J. T. *Tetrahedron* **2003**, *59*, 1837–1857.
(43) Keasey, A.; Mann, B. E.; Yates, A.; Maitlis, P. M. *J. Organomet. Chem.* **1978**, *152*, 117–123.
(44) Hoogervorst, W. J.; Koster, A. L.; Lutz, M.; Spek, A. L.; Elsevier, C. J. *Organometallics* **2004**, *23*, 1161–1164.

X is a mixture of Br and Cl. This process seems to be sped up when a solution of [**2H(PtX(NCN))$_4$**] is subjected to ambient light, but also occurs in its absence. To obtain a pure product, [**2H(PtX(NCN))$_4$**] was converted into the corresponding tetrachloride complex [**2H(PtCl(NCN))$_4$**]. Halide exchange on NCN-pincer platinum halide complexes is usually accomplished by halide abstraction with $AgBF_4$ followed by treatment with a halide source. Unfortunately, treatment of a solution of [**2H(PtX(NCN))$_4$**] in CH_2Cl_2 with $AgBF_4$ led to the formation of a sticky precipitate, which could not be analyzed and did not redissolve upon treatment with LiCl or NaCl. Therefore, [**2H(PtX(NCN))$_4$**] was treated several times with aqueous NH_4Cl in the presence of ambient light, which finally gave [**2H(PtCl(NCN))$_4$**] in an overall yield of 67%.

Palladation of the peripheral ligand sites of [**2H(Br(NCN))$_4$**] was achieved with use of $[Pd_2dba_3]\cdot CHCl_3$ in benzene, to give [**2H(PdBr(NCN))$_4$**] in 90% yield (Scheme 3). Although the solubility profile of this compound is identical with that of [**2H(PtX(NCN))$_4$**], halide exchange in chlorinated solvents is sufficiently slow to allow its isolation as an analytically pure compound. In fact, substantial amounts of halide exchange were only visible after exposure of a $CDCl_3$ solution to ambient light for several days. Exchange of the bromide ligands for chloride ligands via the $AgBF_4$ route led to similar problems as for [**2H(PtX(NCN))$_4$**], while the NH_4Cl route employed in the synthesis of [**2H(PtCl(NCN))$_4$**] did not proceed to completion. Therefore, the compound was fully characterized as the tetrakis-PdBr product.

Unfortunately, nickelation of the peripheral pincer sites with $Ni(COD)_2$ in THF[14] did not lead to the desired product. Although strict anaerobic procedures were employed, the high sensitivity of the NCN-pincer nickel(II) complex toward oxygen in combination with the close proximity of the porphyrin might have facilitated (partial) oxidation of the anticipated [**2H(NiBr(NCN))$_4$**] product.

The selectivities of the palladation and platination reactions for the peripheral NCN-pincer ligand sites were corroborated by ^{1}H NMR spectroscopy. Similar ratios between the integrals corresponding to the benzylic and pyrrolic protons were found for the parent [**2H(Br(NCN))$_4$**] ligand and for the oxidative addition products [**2H(PdBr(NCN))$_4$**] and[**2H(PtCl(NCN))$_4$**]. The selectivity was further supported by mass spectrometry and UV/vis analysis of the products.

To arrive at the targeted heterobimetallic complexes, it was subsequently attempted to introduce metals in the porphyrin core of [**2H(PdBr(NCN))$_4$**] and [**2H(PtCl(NCN))$_4$**]. In order to later use ^{195}Pt NMR spectroscopy as a tool to study the influence of the porphyrin on the peripheral metal centers, it was anticipated that core metalation with metals that would give rise to diamagnetic metalloporphyrins would be of interest. Reactions of [**2H(PdBr(NCN))$_4$**] and [**2H(PtCl(NCN))$_4$**] with $Ni(OAc)_2\cdot 4H_2O$[45] or $Zn(OAc)_2\cdot 2H_2O$[45] in $MeOH/CH_2Cl_2$ only gave moderate yields (~30% isolated yield). Unfortunately, reactions with sources of the 4d and 5d metals, which usually readily give access to the corresponding metalloporphyrins, did not succeed either: treatment of [**2H(PdBr(NCN))$_4$**] or [**2H(PtCl(NCN))$_4$**] with $Ru_3(CO)_{12}$ in 1,2-dichlorobenzene,[46] $[Au(tht)_2]BF_4$ in CH_2Cl_2,[47] or $Pd(OAc)_2$ in $CHCl_3$ did not lead to the formation of the respective porphyrin chelates. We next turned our attention to porphyrin metalation prior to pincer metalation.

Selective Core Metalation. Nickel(II) and zinc(II) could be selectively introduced in the porphyrin part of [**2H(Br(NCN))$_4$**]. Nickel(II) was introduced by using $Ni(acac)_2$ in boiling toluene,[48] which gave [**Ni(Br(NCN))$_4$**] in quantitative yield after recrystallization from hexanes. The introduction of zinc(II) was performed with $Zn(OAc)_2\cdot 2H_2O$ in a mixed solvent system of MeOH and CH_2Cl_2, which readily gave [**Zn(Br(NCN))$_4$**] in 99% yield (Scheme 3). Both compounds were fully characterized and their structures were also confirmed by single-crystal X-ray crystallography. Whereas the introduction of Zn(II) and Ni(II) in [**2H(Br(NCN))$_4$**] proceeded smoothly, attempts to introduce the 4d and 5d metals mentioned above also failed in this case. Zinc porphyrin [**Zn(Br(NCN))$_4$**] was found to form infinite coordination polymers through hexacoordination of the zinc atom including bis(apical) coordination of dimethylamino groups of adjacent [**Zn(Br(NCN))$_4$**] molecules. The resulting solid state topology is of interest with respect to the structures of biological photosynthetic systems[49,50] and has recently been described by us in detail.[51]

Single crystals of [**Ni(Br(NCN))$_4$**] were grown by slow concentration of a saturated solution in *n*-hexane. The crystal structure shows that the nickel(II) ion is located on an exact, crystallographic inversion center at the midpoint of the N_4 coordination plane formed by the pyrrolic nitrogen atoms, with $N_{pyrrole}-Ni$ distances of 1.947(4) and 1.951(4) Å for Ni−N1 and Ni−N2, respectively (Figure 3).

Whereas in most cases the incorporation of the small Ni(II) ion in the porphyrin cavity leads to nonplanar distortions of the macrocycle in order to accommodate it,[52−58] this structure is one of the few examples wherein a planar conformation is observed.[59,60] Contrary to its zinc(II) counterpart, [**Ni(Br(NCN))$_4$**] does not form supramolecular aggregates through intermolecular interactions of the nickel

(45) Padmaja, K.; Wei, L.; Lindsey, J. S.; Bocian, D. F. *J. Org. Chem.* **2005**, *70*, 7972–7978.

(46) Poriel, C.; Ferrand, Y.; Juillard, S.; Le Maux, P.; Simonneaux, G. *Tetrahedron* **2004**, *60*, 145–158.

(47) Chambron, J.-C.; Heitz, V.; Sauvage, J.-P. *New J. Chem.* **1997**, *21*, 237–240.

(48) Senge, M. O.; Gerstung, V.; Ruhlandt-Senge, K.; Runge, S.; Lehmann, I. *J. Chem. Soc., Dalton Trans.* **1998**, 4187–4200.

(49) Balaban, T. S. *Acc. Chem. Res.* **2005**, *38*, 612–623.

(50) Huijser, A. M.; Suijkerbuijk, B. M. J. M.; Klein Gebbink, R. J. M.; Savenije, T. J.; Siebbeles, L. D. A. *J. Am. Chem. Soc.* **2008**, *130*, 2485–2492.

(51) Suijkerbuijk, B. M. J. M.; Tooke, D. M.; Spek, A. L.; van Koten, G.; Klein Gebbink, R. J. M. *Chem. Asian J.* **2007**, *2*, 889–903.

(52) Golder, A. J.; Milgrom, L. R.; Nolan, K. B.; Povey, D. C. *J. Chem. Soc., Chem. Commun.* **1987**, 1788–1789.

(53) Golder, A. J.; Nolan, K. B.; Povey, D. C.; Traylor, T. G. *Inorg. Chim. Acta* **1988**, *143*, 71–75.

(54) Hayvali, M.; Gunduz, H.; Gunduz, N.; Kilic, Z.; Hokelek, T. *J. Mol. Struct.* **2000**, *525*, 215–226.

(55) La, T.; Richards, R. A.; Lu, R. S.; Bau, R.; Miskelly, G. M. *Inorg. Chem.* **1995**, *34*, 5632–5640.

(56) Maclean, A. L.; Foran, G. J.; Kennedy, F. J.; Turner, P.; Hambley, T. W. *Aust. J. Chem.* **1996**, *49*, 1273–1278.

(57) Nurco, D. J.; Smith, K. M.; Fajer, J. *Chem. Commun.* **2002**, 2982–2983.

(58) Richard, P.; Rose, E.; Boitrel, B. *Inorg. Chem.* **1998**, *37*, 6532–6534.

(59) Boyd, P. D. W.; Burrell, A. K.; Campbell, W. M.; Cocks, P. A.; Gordon, K. C.; Jameson, G. B.; Officer, D. L.; Zhao, Z. *Chem. Commun.* **1999**, 637–638.

(60) Sugiura, K.-I.; Iwasaki, K.; Umishita, K.; Hino, S.; Ogata, H.; Miyajima, S.; Sakata, Y. *Chem. Lett.* **1999**, 841–842.

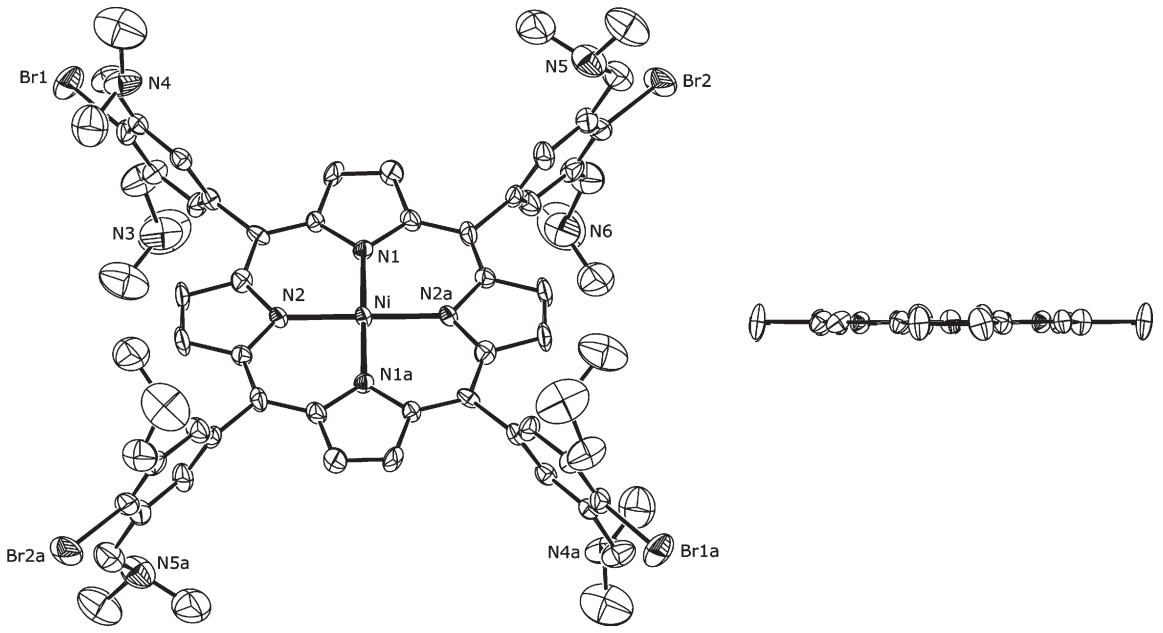

FIGURE 3. ORTEP plot of [**Ni**(**Br**(NCN))$_4$] in the crystal with displacement ellipsoids at the 50% probability level (left). Hydrogen atoms and disordered solvent molecules have been omitted for clarity. Symmetry operation a: $-x$, $1-y$, $1-z$. On the right is depicted a view along the N1a−Ni−N1 direction, wherein all *meso*-phenyl groups have been omitted.

atom with NMe_2 groupings[61] of neighboring [**Ni**(**Br**(NCN))$_4$] molecules.

Heteromultimetallic Systems. To arrive at the targeted heteromultimetallic systems [**M^1**(**M^{2}X**(NCN))$_4$] (M^1 = Ni, Zn; M^{2}X = PdBr, PtCl), the core-metalated porphyrins [**Ni**(**Br**(NCN))$_4$] and [**Zn**(**Br**(NCN))$_4$] were peripherally metalated with palladium and platinum according to the procedures employed for [**2H**(**PdBr**(NCN))$_4$] and [**2H**(**PtCl**(NCN))$_4$] (vide supra). Peripheral palladation of [**Ni**(**Br**(NCN))$_4$] and [**Zn**(**Br**(NCN))$_4$] proceeded readily with a slight excess of [Pd_2dba_3]·$CHCl_3$ in benzene at room temperature (Scheme 3). The resulting peripherally palladated pincer−porphyrin hybrids [**Ni**(**PdBr**(NCN))$_4$] and [**Zn**(**PdBr**(NCN))$_4$] were isolated as analytically pure compounds in high yields. The corresponding tetraplatinated compounds [**Ni**(**PtCl**(NCN))$_4$] and [**Zn**(**PtCl**(NCN))$_4$] were obtained after treatment with [Pt_2dipdba$_3$] in refluxing benzene followed by halide exchange with NH_4Cl. In the case of [**Ni**(**PtCl**(NCN))$_4$], the Br/Cl exchange could also be achieved by treatment with $AgBF_4$ and LiCl, most probably owing to the relative inertness of nickel porphyrins.

Clear evidence for the 4-fold oxidative addition of the pincer−(metallo)porphyrin hybrids [**M^1**(**Br**(NCN))$_4$] (M^1 = 2H, Ni, Zn) to Pd(0) and Pt(0) (to give the corresponding *meso*-tetrakis(NCN-pincer MX) complexes [**M^1**(**M^{2}X**(NCN))$_4$]) was obtained from a comparison of their ^{1}H NMR spectra. Whereas the benzylic protons and the dimethylamino-protons of the ligands resonate at $\delta \approx 3.8$ and 2.4 ppm, respectively, they are shifted to $\delta \approx 4.2$ and 3.2 ppm upon coordination of the nitrogen atoms to the metal. Peripheral metalation of [**Zn**(**Br**(NCN))$_4$] was especially clear because the four broad resonances of the starting material (caused by self-aggregation through intermolecular Zn−N bonds) became sharp after intramolecular coordination of the dimethylamino groups to Pd or Pt. Halide scrambling at the metal centers (Br/Cl) was observed in all cases after long reaction times in chlorinated solvents such as CH_2Cl_2 or $CHCl_3$. This transformation was inferred from both ^{1}H NMR spectroscopy and (MA)LDI-TOF mass spectrometry. In the ^{1}H NMR spectrum all peaks for the chloride and bromide complexes coincide except for the signals belonging to the NMe_2 protons. In the case where X = Cl those signals are shifted ~0.04 ppm upfield with respect to the case where X = Br. For all complexes, mass spectrometric analyses were performed by MALDI-TOF (with 2,5-dihydroxybenzoic acid as matrix or without matrix). In every case, peaks corresponding to the molecular ion were found. Additional information about the composition of the [**M^1**(**M^{2}X**(NCN))$_4$] compounds was obtained by the fragmentation pattern of the molecular ion. Each molecular ion peak ([MI]$^+$) was accompanied by peaks corresponding to loss of one halide ([MI − X]$^+$), one metallohalide group ([MI − M^{2}X]$^+$), one halide and one metallohalide group ([MI − M^{2}X − X]$^+$), and so forth. When MALDI-TOF samples of [**M^1**(**PdBr**(NCN))$_4$] were prepared in CH_2Cl_2 the peaks corresponding to (partially) halogen-scrambled complexes were always found.

Single crystals of the pyridine adduct of [**Zn**(**PdBr**(NCN))$_4$], {[**Zn**(**PdBr**(NCN))$_4$](**pyridine**)}, were obtained by slow evaporation of a solution of [**Zn**(**PdBr**(NCN))$_4$] in a mixed solvent system comprising CH_2Cl_2, hexanes, and one drop of pyridine. The molecular structure as obtained by X-ray crystallography is depicted in Figure 4. It comprises a [*meso*-tetraphenylporphyrinato]zinc(II) unit of which the zinc(II) ion is pentacoordinate in a distorted tetragonal pyramidal fashion.

The structure does not contain any symmetry elements. The four pyrrolic nitrogen atoms of the porphyrin form the basal plane with Zn−N pyrrole distances ranging from

(61) Jia, S.-L.; Jentzen, W.; Shang, M.; Song, X.-Z.; Ma, J.-G.; Scheidt, W. R.; Shelnutt, J. A. *Inorg. Chem.* **1998**, *37*, 4402–4412.

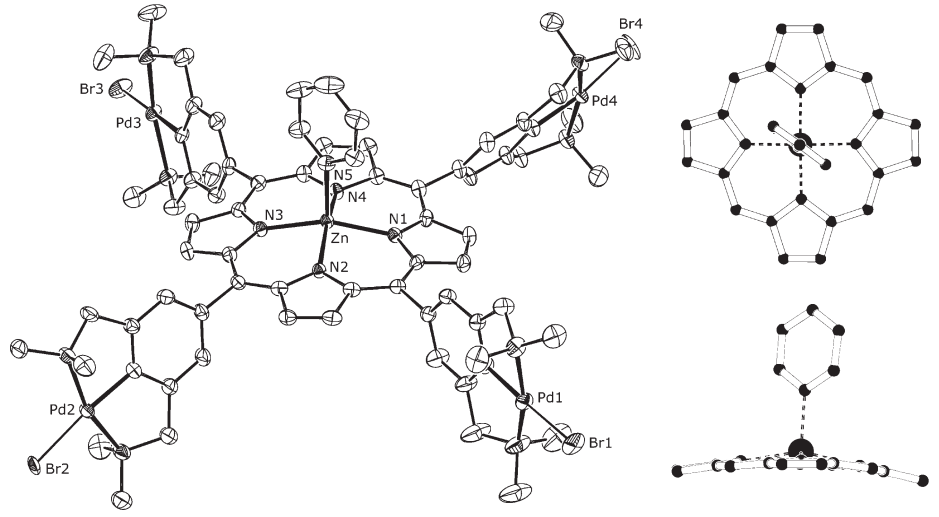

FIGURE 4. ORTEP plot of {[**Zn**(**PdBr**(**NCN**))$_4$](**pyridine**)} in the crystal with displacement ellipsoids at the 50% probability level. Hydrogen atoms and solvent molecules ($CHCl_3$ and toluene) present in the crystal lattice have been omitted for clarity. On the right are shown a view along the N5−Zn axis (top) and along the N2−N4 axis (bottom).

2.072(3) to 2.082(3) Å. The nitrogen atom of a pyridine molecule occupies the apical fifth ligand position at 2.100(3) Å from the zinc atom, which is displaced from the least-squares plane of the porphyrin by 0.3927(4) Å toward the pyridine molecule. The Zn−N5 distance compares to the literature values for ZnTPP-$N_{pyridine}$ adducts, which cover quite a broad range between 2.10 and 2.20 Å.[62−66] The four *meso*-phenyl groups are all part of an NCN-pincer bromidopalladio(II) moiety with the Pd atoms at the positions para with respect to the porphyrin ring. The Pd−Pd distances across the porphyrin structure amount to 19.035(5) Å for Pd1−Pd3 and 19.055(5) Å for Pd2−Pd4, respectively. Each distorted square-planar Pd(II) center is ligated by a κ^3-coordinating NCN-pincer moiety provided by the pincer−porphyrin hybrid and by a halide ion at the position trans with respect to the Pd−C σ-bond. The halide position was refined with a partial occupation by chloride (54%) and by bromide (46%). The Pd−C_{ipso} distances are in the range of 1.905(3) to 1.924(4) Å. The benzylic nitrogen atoms reside at distances of 2.090(3)−2.111(3) Å from the Pd atoms. The *meso*-phenyl groups are connected to the porphyrin at angles ranging from 58.45(16)° to 84.57(16)°.

II. Spectroscopic and Physicochemical Characterization. There are several ways to probe intramolecular interaction in the present [$\mathbf{M^1(M^2X(NCN))_4}$] molecules, since the (metallo)porphyrin and the NCN-pincer metallohalide each display their own characteristic responses to external stimuli. The intramolecular influence of the (metallo)porphyrin part and the NCN-pincer PtCl moieties on each other was studied by means of ^{195}Pt NMR spectroscopy and UV/vis spectroscopy. Additionally, it was also examined by means of its chemical reactivity, i.e., selective pyridine binding to zinc porphyrin moieties and selective SO_2 and $CuCl_2$ reactivity toward the NCN-pincer platinum groups.

TABLE 1. ^{195}**Pt NMR Chemical Shifts for [2H(PtCl(NCN))$_4$], [Ni(PtCl(NCN))$_4$], and [Zn(PtCl(NCN))$_4$]**[a]

compd	δ_{Pt} (ppm)
[**2H**(**PtCl**(**NCN**))$_4$]	−3162
[**Ni**(**PtCl**(**NCN**))$_4$]	−3170
[**Zn**(**PtCl**(**NCN**))$_4$]	−3176
[PtCl(NCN)]	−3147

[a]Chemical shifts were referenced to an external standard (1 M $Na_2[PtCl_6]$ in D_2O) before each measurement.

^{195}Pt NMR Spectroscopy. In general, the ^{195}Pt nucleus is highly sensitive to changes in its magnetic environment.[67] Particularly in para-substituted NCN-pincer PtX complexes ([PtX(NCN-Z)]), the ^{195}Pt chemical shift has been proven to be highly sensitive to either the electron-releasing or -withdrawing properties of the para-substituent Z.[16,68] In the current systems, the para-substituent of each NCN-pincer PtX group is a (metallo)porphyrin. The electronic properties of the latter are strongly dependent on the complexed metal[29] and thus it was investigated whether the nature of the central (metallo)porphyrin influences the chemical shift of the peripheral Pt centers in our hybrids. ^{195}Pt NMR spectra were recorded of [$\mathbf{M^1(PtCl(NCN))_4}$] ($M^1$ = 2H, Ni, Zn) and their δ_{Pt} values are listed in Table 1 (samples were measured at different concentrations (2−10 mM) and it was found that for each compound $\Delta\delta_{Pt} < 1$ ppm within this concentration range). Whereas the differences between the δ_{Pt} values of these compounds are relatively small, they are detectable and reproducible and, therefore, indicate a difference in the electron density at Pt as a direct consequence of a change in the porphyrin metal. In comparison with the *p*-H-substituted [PtCl(NCN)], the (metallo)porphyrins cause an upfield shift of the Pt nuclei of the peripheral NCN-pincer platinum systems.

(62) Boyd, P. D. W.; Hosseini, A. *Acta Crystallogr.* **2006**, *E62*, m1542–m1544.
(63) D'Souza, F.; Rath, N. P.; Deviprasad, G. R.; Zandler, M. E. *Chem. Commun.* **2001**, 267–268.
(64) Kleij, A. W.; Reek, J. N. H. *Chem.—Eur. J.* **2006**, *12*, 4218–4227.
(65) Shukla, A. D.; Dave, P. C.; Suresh, E.; Das, A.; Dastidar, P. *J. Chem. Soc., Dalton Trans.* **2000**, 4459–4463.
(66) Kleij, A. W.; Kuil, M.; Tooke, D. M.; Spek, A. L.; Reek, J. N. H. *Inorg. Chem.* **2005**, *44* (22), 7696–7698.
(67) Priqueler, J. R. L.; Butler, I. S.; Rochon, F. D. *Appl. Spectrosc. Rev.* **2006**, *41*, 185–226.
(68) Albrecht, M.; Rodríguez, G.; Schoenmaker, J.; van Koten, G. *Org. Lett.* **2000**, *2* (22), 3461–3464.

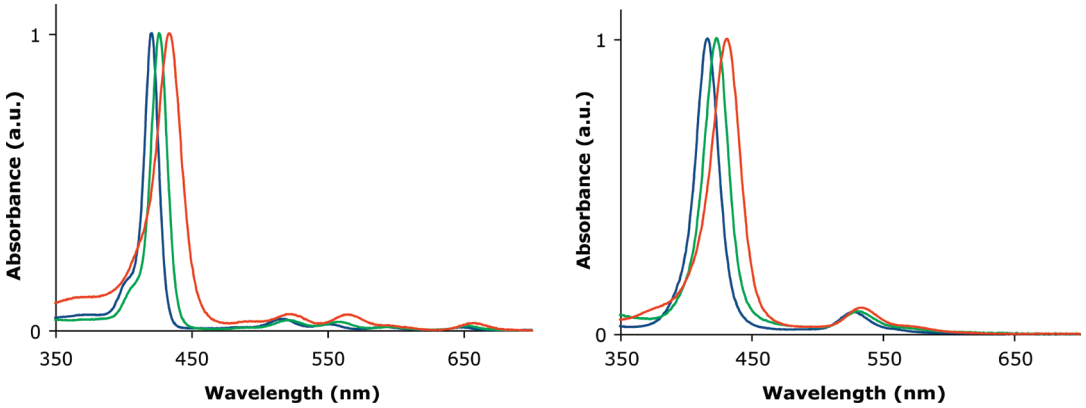

FIGURE 5. Comparison of the normalized (Soret band) electronic spectra of [M^1(**Br**(NCN))$_4$] (blue), [M^1(**PdBr**(NCN))$_4$] (green), and [M^1(**PtCl**(NCN))$_4$] (red) for the M^1 = 2H (left) and M^1 = Ni (right) complexes.

Along the series M^1 = 2H, Ni, Zn, the Pt nuclei gradually become more shielded. Similarly, the porphyrin part of the molecule becomes a better electron donor along the same series by virtue of an increasing destabilization of its HOMO (from ca. −11.7 and ca. −11.0 eV for the free-base and the nickel complex, respectively, to ca. −10.6 eV in the case of zinc).[69] This trend follows the redox potentials of the corresponding tetraphenylporphyrin (TPP) complexes as a measure of the porphyrin ring's electron-donating power. Hence, these values indicate that the electron density on the porphyrin increases in the order of M^1 = 2H < Ni < Zn [$E_{1/2}$(0/1) = 0.97, 0.95, and 0.71 V, respectively].[70]

UV/Vis Spectroscopy. The electronic spectra of (metallo)porphyrins are dominated by the high energy Soret (B) band and lower energy Q bands. The energies of the transitions are largely governed by the incorporated metal and by the substitution pattern at the porphyrin periphery. For *meso*-tetrakis(aryl)porphyrins, it is known that these energies are also dependent on the electronic properties of the *meso*-aryl groups, i.e., on the nature of their substituents.[71−77] It was therefore expected that a possible influence of the peripheral NCN-metallopincer groups of [M^1(M^2X(NCN))$_4$] on the (metallo)porphyrin core could be deduced from their UV/vis spectra. Figure 5 shows the UV/vis absorption spectra of the 2H- (left) and Ni-series (right) of [M^1(M^2X(NCN))$_4$], respectively. For these series, the spectra of the [M^1(**Br**(NCN))$_4$] species were very similar to those of the corresponding TPP analogues. When Pd was incorporated at the peripheral NCN-ligand sites, however, bathochromic shifts, amounting to 5 nm for [**2H**(**PdBr**(NCN))$_4$], 6 nm for [**Ni**(**PdBr**(NCN))$_4$], and 2 nm for [**Zn**(**PdBr**(NCN))$_4$], were observed. The Q-bands also shifted bathochromically and increased in intensity with respect to the Soret band. For peripheral platination the effects are even more pronounced: the absolute bathochromic shifts in comparison with the nonperipherally metalated pincer porphyrin hybrids are 13, 14, and 9 nm for [**2H**(**PtCl**(NCN))$_4$], [**Ni**(**PtCl**(NCN))$_4$], and [**Zn**(**PtCl**(NCN))$_4$], respectively. With respect to the corresponding Pd compounds the differences are 8, 8, and 7 nm. It was noted that exchange of peripheral bromide ligands for chloride in [**Ni**(**PtCl**(NCN))$_4$] had no significant effect on its electronic spectrum.

Pyridine Binding at Zinc. Pyridine is known to bind to zinc(II) porphyrins to give distorted square-pyramidal coordination complexes.[78] The binding constant of this interaction depends on the interaction of an unoccupied molecular orbital with zinc character on the porphyrin with the pyridine lone pair.[79] The binding constants of pyridine with [tetraphenylporphyrinato]zinc(II) (ZnTPP),[80] [**Zn**(**PdBr**(NCN))$_4$], and [**Zn**(**PtCl**(NCN))$_4$] in CH_2Cl_2 at room temperature were determined by UV/vis spectroscopy (Figure 6).

For ZnTPP a binding constant of 8100 ± 200 M^{-1} was determined, which corresponds well with the value found by Mizutani et al. (7720 M^{-1}).[81] Interestingly, the binding constants decreased substantially upon peripheral metalation: for [**Zn**(**PdBr**(NCN))$_4$], a value of 6000 ± 200 M^{-1} was found, whereas [**Zn**(**PtCl**(NCN))$_4$] exhibits an even lower affinity for pyridine at 4700 ± 150 M^{-1}. These findings indicate that peripheral metalation of the NCN-pincer groups in the hybrids destabilizes the unoccupied orbital with zinc character of their porphyrin moieties. This effect is larger in the case when platinum occupies the peripheral positions than when palladium does.

Reactions at Pt. The experiments described above demonstrate that there is an electronic interaction between the peripheral metallopincer groups and the central porphyrin

(69) Gouterman, M., In *The Porphyrins*; Dolphin, D., Ed.; Academic Press, Inc.: New York, 1978; Vol. 3.
(70) Führhop, J.-H. *Reversible Reactions of Porphyrins and Metalloporphyrins*; Elsevier Scientific Publishing Company: Amsterdam, The Netherlands, 1974.
(71) Chang, D.; Malinski, T.; Ulman, A.; Kadish, K. M. *Inorg. Chem.* **1984**, *23*, 817–824.
(72) Foran, G. J.; Armstrong, R. S.; Crossley, M. J.; Lay, P. A. *Inorg. Chem.* **1992**, *31*, 1463–1470.
(73) Jones, R. D.; Summerville, D. A.; Basolo, F. *J. Am. Chem. Soc.* **1978**, *100* (14), 4416–4424.
(74) Kadish, K. M.; Morrison, M. M. *Inorg. Chem.* **1976**, *15* (4), 980–982.
(75) Walker, F. A.; Beroiz, D.; Kadish, K. M. *J. Am. Chem. Soc.* **1976**, *98* (12), 3484–3489.
(76) Ghosh, A. *J. Am. Chem. Soc.* **1995**, *117*, 4691–4699.
(77) Ghosh, A. *J. Mol. Struct.* **1995**, *388*, 359–363.
(78) Hambright, P. Dynamic Coordination Chemistry of Metalloporphyrins. In *Porphyrins and Metalloporphyrins*; Smith, K. M., Ed.; Elsevier Scientific Publishing Company: Amsterdam, The Netherlands, 1975; pp 259−263 and references cited therein.
(79) D'Souza, F.; Deviprasad, G. R.; Zandler, M. E.; Hoang, V. T.; Klykov, A.; VanStipdonk, M.; Perera, A.; El-Khouly, M. E.; Fujitsuka, M.; Ito, O. *J. Phys. Chem. A* **2002**, *106*, 3243–3252.
(80) ZnTPP was used as a model compound for [**Zn**(**Br**(NCN))$_4$], since the latter's coordination behavior with pyridine is obscured by a competing, intermolecular Zn-NMe_2R self-assembly process (ref 51).
(81) Mizutani, T.; Wada, K.; Kitagawa, S. *J. Org. Chem.* **2000**, *65*, 6097–6106.

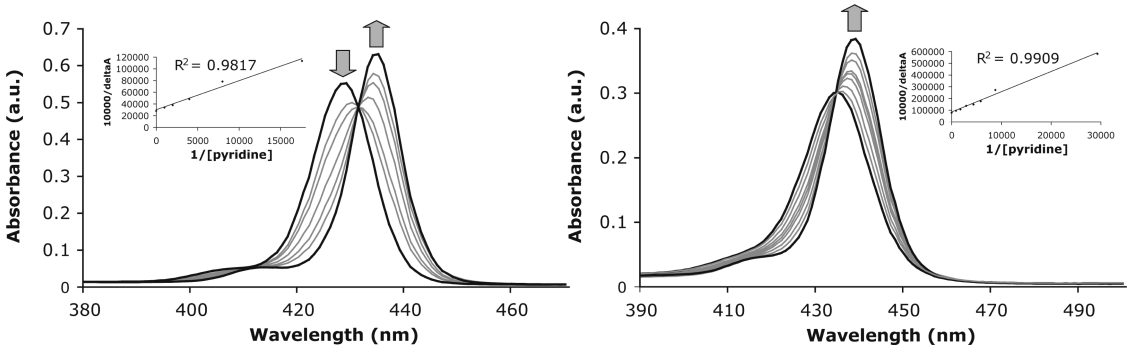

FIGURE 6. Spectral changes of solutions of [**ZnPdBr(NCN)**$_4$] (left) and [**Zn(PtCl(NCN)**$_4$] upon titration with pyridine. The insets show the corresponding Benesi−Hildebrand plots.

SCHEME 4. Reactions Performed on NCN-Pincer PtCl Sites[a]

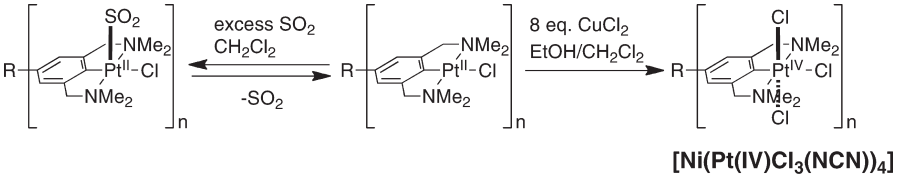

[a] n = 4, R = [porphyrinato]metal(II)-5,10,15,20-tetrayl (metal = 2H, Ni, Zn).

group. The rich chemistry of the NCN-pincer Pt species prompted us to investigate the effect of chemistry at the peripheral NCN-pincer PtCl sites on the UV/vis spectra of the porphyrin core.

Gaseous SO_2 is known to bind to NCN-pincer Pt halide complexes via a Lewis base/Lewis acid interaction in which Pt acts as the Lewis base (through its filled d_{z^2} orbital) and SO_2 as the Lewis acid (Scheme 4). During this transformation, a diagnostic color change from colorless to orange occurs, which led to the use of these complexes as SO_2 sensors.[82]

Whereas the electronic spectra of all [**M**^{1}**(Br(NCN))**$_4$] compounds are completely insensitive to the presence of an excess of SO_2 ($\Delta\lambda_{max}$ < 0.1 nm), dissolution of [**M**^{1}**(PtCl(NCN))**$_4$] in a saturated CH_2Cl_2 solution of SO_2 leads to an immediate change in λ_{max} of the Soret band leading to hypsochromic shifts of ~4 nm with concomitant broadening of the band. Color changes of the solutions were not observed due to the intense absorption bands of the porphyrins in the visible. The two UV/vis absorption bands of the NCN-pincer PtCl-SO_2 complex itself [$\lambda_{max} \approx 350$ nm ($\varepsilon \approx 7000$ M^{-1} cm^{-1}), 410 ($\varepsilon \approx 2000$ M^{-1} cm^{-1})][83] were not observed; most probably they are obscured by the dominant Soret band. Upon decomplexation of SO_2 and subsequent evaporation from the sample, the Soret band returned to its initial position. The complexation/decomplexation could be repeated numerous times, without a change in the response of the system, suggesting the process is reversible.

In addition to the reversible reaction of the NCN-pincer PtCl groups with SO_2, we also explored the irreversible reaction of the peripheral platinum pincer centers with $CuCl_2$ in a mixture of CH_2Cl_2 and EtOH,[84] which gave the almost insoluble [**Ni(Pt(IV)Cl**$_3$**(NCN))**$_4$] species. Conversion of the Pt(II) centers into Pt(IV) centers exerts a dramatic effect on the electronic spectrum of the hybrid (Figure 7). The Soret band exhibits a substantial hypsochromic shift of 12 nm when the peripheral NCN-pincer Pt(II)Cl sites are irreversibly oxidized to NCN-Pt(IV)Cl_3. Control experiments with NiTPP showed no reactivity toward $CuCl_2$. Unfortunately, the same reaction could not be applied to [**2H(PtCl(NCN))**$_4$] and [**Zn(PtCl(NCN))**$_4$] due to side reactions, which were not investigated further.

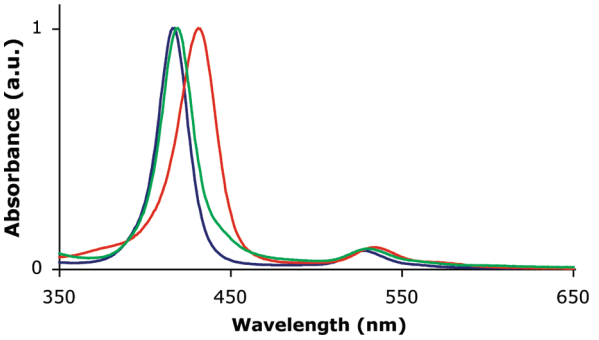

FIGURE 7. Comparison of the normalized electronic spectra of [**Ni(Br(NCN))**$_4$] (blue), [**Ni(PtCl(NCN))**$_4$] (red), and [**Ni(Pt(IV)Cl**$_3$**(NCN))**$_4$] (green).

Discussion

I. Synthesis. We have previously described the synthesis of [**2H(H(NCN))**$_4$],[33] whose selective 4-fold metalation at the phenyl-positions para with respect to the porphyrin ring

(82) Albrecht, M.; Lutz, M.; Spek, A. L.; van Koten, G. *Nature* **2000**, *406*, 970–974.

(83) Albrecht, M.; Gossage, R. A.; Lutz, M.; Spek, A. L.; van Koten, G. *Chem.—Eur. J.* **2000**, *6*, 1431–1445.

(84) Terheijden, J.; van Koten, G.; de Booys, J. L.; Ubbels, H. J. C.; Stam, C. H. *Organometallics* **1983**, *2*, 1882–1883.

[ortho with respect to both (dimethylamino)methyl donor groupings] should give direct access to the family of [$\mathbf{M^1(M^2X(NCN))_4}$] hybrid compounds described here. Among other reasons, we anticipated that this strategy would be hampered by the selectivity of a direct cyclopalladation reaction for the positions meta with respect to the desired para position.[85] An alternative route to arrive at [$\mathbf{M^1(M^2X(NCN))_4}$] via [$\mathbf{2H(H(NCN))_4}$] would involve a lithiation/transmetalation sequence.[13,86] This idea was abandoned for a number of reasons. First of all, it would involve a protection step of the porphyrin ring (metalation) prior to lithiation/transmetalation and, to obtain the free-base porphyrin, an inevitable deprotection step (demetalation) thereafter. The conditions used for demetalation of the porphyrin ring can also lead to demetalation of the NCN-metallopincer fragment, especially in the case when the metal in the pincer unit is palladium. In addition, the necessary equimolarity of organolithium reagent and NCN-pincer fragment is generally difficult to achieve practically[87] as a result of the small quantities in which [$\mathbf{2H(H(NCN))_4}$] is available. Therefore, a different route that relies on metalation of the NCN-pincer fragments via oxidative addition was opted for.[13] This requires the presence of a group that can oxidatively add to Pd or Pt centers, e.g., a carbon−bromine bond.[13] However, if M(II) sources (M = Pd, Pt) are used in combination with a free-base porphyrin, metalation of the porphyrin may also occur.[31] For example, when [$\{Pt(p\text{-tol})_2SEt_2\}_2$] in benzene[88] was used as a platinating agent[16] for [$\mathbf{2H(Br(NCN))_4}$], not only the NCN-pincer groups were platinated but also the porphyrin core. This was independently confirmed by the reaction of tetraphenylporphyrin (TPP) with half an equivalent of [$\{Pt(p\text{-tol})_2SEt_2\}_2$] in refluxing benzene. After 3 h at reflux, the crude reaction mixture consisted of 55% TPP, 38% PtTPP,[89] and 7% of an unidentified, platinated porphyrin. The peripheral metalation reactions of [$\mathbf{2H(Br(NCN))_4}$] were eventually performed with the M(0) complexes [$Pd_2(dba)_3]\cdot CHCl_3$ and [$Pt_2dipdba_3$]. This strategy readily yields the desired peripherally metalated porphyrins [$\mathbf{2H(M^2X(NCN))_4}$] without affecting the central porphyrin cavity.

In analogy to the *meso*-metalated porphyrins of Arnold et al.[27] heteromultimetallic complexes derived from [$\mathbf{2H(Br(NCN))_4}$] can be synthesized in two ways in which either the porphyrin or the pincer is metalated before the other. Whereas the selectivity and yield of the palladation and platination reactions at the periphery were always high, metalation of the porphyrin cavity after peripheral metalation sometimes led to the formation of side products. For example, when [$\mathbf{2H(PtCl(NCN))_4}$] was reacted with $Ni(OAc)_2\cdot 4H_2O$ in a mixture of CH_2Cl_2/MeOH at 40 °C,[90] ^{1}H NMR analysis of the product mixture showed substantial amounts of unidentified impurities. The impurities composed 50% of the total and could be removed by column chromatography. Mass spectrometry and ^{1}H NMR unfortunately did not provide conclusive evidence as to their nature. Although to a lesser extent, the same outcome was noted when attempting to introduce Zn(II) into the platinated porphyrin. A metalation sequence in which the porphyrin is metalated prior to the peripheral pincer ligands was therefore used for the synthesis of heterobimetallic hybrids [$\mathbf{M^1(M^2X(NCN))_4}$].

After the peripheral metalation steps, analysis of the products obtained after a workup involving solubilization in chlorinated solvents (CH_2Cl_2, $CHCl_3$) revealed that halide scrambling took place at the peripheral metal atoms (Br/Cl). We found that this process is much faster for the peripherally platinated porphyrins than for their palladium analogues. The [$\mathbf{M^1(PdBr(NCN))_4}$] complexes could be readily isolated as analytically pure solids; halide scrambling only took place when solutions were exposed to ambient light for several days (as judged from ^{1}H NMR spectroscopy). For the platinum compounds [$\mathbf{M^1(PtX(NCN))_4}$], however, this exchange reaction proved to be very fast. Even in degassed and deacidified solutions, and with a minimum exposure to light, halide scrambling always seemed to take place. For their novel *meso*-η^1-metalloporphyrins,[21−24,26,27] Arnold et al. also found that halide exchange occurred in chlorinated solvents. They ascribed this to the high trans-effect of the σ-bound porphyrin ligand.[21] Although this might be a viable explanation, reference experiments conducted by us on the parent NCN-pincer PdBr and PtBr compounds showed that these complexes underwent halide scrambling much more slowly, if at all, than the corresponding multimetallic pincer−porphyrin hybrids. This observation would make a trans-effect explanation quite drastic and rather seems to point to another effect of the porphyrin on halide exchange at the pincer−metal sites. Recently, Perutz et al. found that photoinduced electron transfer from a metalloporphyrin to an intramolecular Re center led to fast ligand exchange at Re.[91−94] This phenomenon might also be of importance when considering halide exchange on palladium and platinum complexes connected to a (metallo)porphyrin system.

II. Intramolecular Influence between the Complexes. The influence of the (metallo)porphyrin on the electronic properties of the peripheral platinum groups was investigated by several means. ^{195}Pt NMR spectroscopy indicated that, for the [$\mathbf{M^1(PtCl(NCN))_4}$] compounds ($M^1$ = 2H, Ni, Zn), the electron density at Pt increases in the order M^1 = 2H < Ni < Zn. Cyclovoltammetric studies on the analogous metal tetraphenylporphyrins have shown that a decrease of the first oxidation potential of the (metallo)porphyrin, i.e., the increase in HOMO energy, follows the same order (vide supra). The correlation between the increments of δ_{Pt} in the [$\mathbf{M^1(PtCl(NCN))_4}$] series and those of $E_{1/2}$ (0/1) of the M^1TPP series shows that the electronic nature of the metalloporphyrin in the hybrids has an effect on the electron

(85) Steenwinkel, P.; Gossage, R. A.; van Koten, G. *Chem.—Eur. J.* **1998**, *4*, 759–762.
(86) Grove, D. M.; van Koten, G.; Louwen, J. N.; Noltes, J. G.; Spek, A. L.; Ubbels, H. J. C. *J. Am. Chem. Soc.* **1982**, *104*, 6609–6616.
(87) Kleij, A. W.; Gossage, R. A.; Klein Gebbink, R. J. M.; Brinkmann, N.; Reijerse, E. J.; Kragl, U.; Lutz, M.; Spek, A. L.; van Koten, G. *J. Am. Chem. Soc.* **2000**, *122*, 12112–12124.
(88) Canty, A. J.; Patel, J.; Skelton, B. W.; White, A. H. *J. Organomet. Chem.* **2000**, *599*, 195–199.
(89) Milgrom, L. R. *Polyhedron* **1984**, *3*, 879–882.
(90) Since the starting material is virtually insoluble in toluene, the $Ni(acac)_2$/toluene procedure could not be employed. In addition, Ni(II) introduction using $Ni(OAc)_2$ is milder and also the nickel(II) insertion into [$\mathbf{2H(Br(NCN))_4}$] using the same method yielded quantitatively [$\mathbf{Ni(Br(NCN))_4}$] without any problems.
(91) Aspley, C. J.; Lindsay Smith, J. R.; Perutz, R. N. *J. Chem. Soc., Dalton Trans.* **1999**, 2269–2271.
(92) Aspley, C. J.; Lindsay Smith, J. R.; Perutz, R. N.; Pursche, D. *J. Chem. Soc., Dalton Trans.* **2002**, 170–180.
(93) Gabrielsson, A.; Hartl, F.; Lindsay Smith, J. R.; Perutz, R. N. *Chem. Commun.* **2002**, 950–951.
(94) Gabrielsson, A.; Hartl, F.; Zhang, H.; Lindsay Smith, J. R.; Towrie, M.; Vlček, J., A.; Perutz, R. N. *J. Am. Chem. Soc.* **2006**, *128*, 4253–4266.

density on the peripheral platinum centers. In fact, the (metallo)porphyrin part acts as an electron donor in these systems.

The absorption maxima as observed in their UV/vis spectra for [**2H**(**Br**(**NCN**))$_4$] and [**Ni**(**Br**(**NCN**))$_4$] parallel those found for their TPP analogues 2HTPP and NiTPP. This shows that the *meso*-3,5-bis[(dimethylamino)methyl]-4-bromophenyl groups exert relatively little electronic influence on the porphyrin chromophores compared to that of phenyl groups. The insertion of palladium or platinum atoms in the carbon−bromine bonds, however, leads to bathochromic shifts in the electronic spectra. The extent to which this occurs for peripheral palladation is 4 nm, while peripheral platination leads to bathochromic shifts amounting to 12 nm, indicating a reduction of the $S_0 \rightarrow S_2$ gap by peripheral metalation. Arnold and co-workers noted similar effects for their *meso*-η^1-palladio(II) and -platino(II) porphyrins, but attributed those to nonplanar distortions of the porphyrin macrocycle (although they did ascribe shifts in the redox potentials of the peripherally metalated porphyrins to the strong electron-donating capacity of the palladium and platinum groups).[21] In our case, distortions of the porphyrin core are not expected upon metalation of the rather remote NCN-pincer ligand sites. For example, the domed structure of the zinc porphyrin part of the crystal structure of {[**Zn**(**PdBr**(**NCN**))$_4$](**pyridine**)} (Figure 4) is not different from those of pyridine adducts of other zinc tetraarylporphyrins.[62,63,65,66] In a related tetrakis(SCS-pincer Pd-Cl)porphyrin, the porphyrin core did not show significant distortions from planarity in comparison with other *meso*-tetraarylporphyrins.[33]

From previous research it is known that metalation of the NCN-pincer ligand fragment leads to release of electron density from the metal to the pincer aryl ring.[16,95] As to the extent of electron-donation of the metal to the *meso*-aryl rings of the pincer−porphyrin hybrids, or electronic coupling between them, Parshall found that MX groups (M = Pd, Pt; X = halide) connected to a σ-phenyl group are electron donating to the aromatic ring and increase the phenyl-HOMO in energy.[96,97] These effects are significantly more pronounced for platinum than for palladium. When these findings are compared to the results presented here, this also accounts for the stronger bathochromic shifts of the Soret bands induced by peripheral platination in comparison with those of peripheral palladation. These interactions likely occur by virtue of interaction between the π-orbitals on the *meso*-phenyl rings and the π-orbitals on the porphyrin core.[76,98] Although single-crystal X-ray analysis has shown that the angles between the *meso*-phenyl rings and the porphyrin range from 58° to 84° (see Figure 4 {[**Zn**(**PdBr**(**NCN**))$_4$](**pyridine**)}), it should be noted that in solution rotation around the carbon−carbon bond connecting the *meso*-phenyls to the porphyrin is still feasible.[99] Hence, this will allow for the occurrence of intramolecular interactions that are mediated through the π-system.

Pyridine binds stronger to zinc tetraarylporphyrins with electron-withdrawing groups than to those with electron-releasing groups. This arises from the fact that electron-withdrawing substituents (e.g., pentafluorophenyl)[100] lower the LUMO with zinc character on the porphyrin, which makes its interaction with the pyridine lone pair energetically more favorable. For our systems the interaction between the pyridine and zinc porphyrin becomes weaker along the series ZnTPP > [**Zn**(**PdBr**(**NCN**))$_4$] > [**Zn**(**PtCl**(**NCN**))$_4$], which points to a destabilization of the unoccupied porphyrin molecular orbital that is responsible for the binding of a ligand to the central zinc atom upon peripheral metalation.

Chemistry that is selective for the NCN-pincer Pt moiety also influences the metalloporphyrin's electronic properties. Upon SO_2 binding to the four peripheral NCN-pincer PtCl moieties of [**Ni**(**PtCl**(**NCN**))$_4$], its Soret band shows a hypsochromic shift of about 4 nm. The oxidation of the platinum(II) centers of [**Ni**(**PtCl**(**NCN**))$_4$] to platinum(IV) has an even stronger effect on the electronic absorption spectrum of the resulting [**Ni**(**Pt**(**IV**)**Cl$_3$**(**NCN**))$_4$]. As a result of this reaction the Soret band almost shifts back to the position of the Soret band of [**Ni**(**Br**(**NCN**))$_4$]. Complexation of SO_2 to the d_{z^2} orbital of platinum is expected to modulate the energies of its other d orbitals, including those interacting with the π-system of the phenyl ring. This apparently leads to a decreased interaction between the porphyrin and the *meso*-phenyl rings by increasing the gap between the interacting energy levels of the platinum center and its phenyl ligand. Oxidation of the platinum centers to Pt(IV) completely alters the orbital system at Pt,[1] which, as inferred from the hypsochromic shift of the Soret band of [**Ni**(**PtCl**(**NCN**))$_4$] as a result of this reaction, apparently leads to even smaller interaction of the porphyrin with the *meso*-phenyl groups.

In another part of our research, we have synthesized and investigated the closely related 5-(3,5-bis[(dimethylamino)-methyl]-4-bromophenyl)-10,15,20-tris(*p*-tolyl)porphyrin and its heterobimetallic complexes.[101] For these complexes, the effects of peripheral palladation, platination, and chemistry on the peripheral NCN-pincer PtCl sites are reduced 4-fold when compared with those of the tetrapincer−porphyrin systems discussed here. These findings demonstrate the cumulativity of the effects exerted by the peripheral metalated pincer groups. Arnold and co-workers noted a similar, additive effect for the incorporation of Pt atoms at one or two *meso*-positions of their *meso*-η^1-metalloporphyrins.[27]

Conclusions

A novel *meso*-tetrakis(NCN-pincer ligand)porphyrin hybrid, [**2H**(**Br**(**NCN**))$_4$], was synthesized via a 13-step procedure in a total yield of 5.3%. By design, orthogonal metalation procedures could be employed to metalate either the pincer or porphyrin moiety. M(II) salts were employed for metal insertion into the tetrapyrrolic macrocyle whereas the M(0) complexes [Pd_2dba_3]·$CHCl_3$ and [$Pt_2dipdba_3$] were used for metalation of the peripheral NCN-pincer ligand

(95) Köcher, S.; van Klink, G. P. M.; van Koten, G.; Lang, H. *J. Organomet. Chem.* **2006**, *691*, 3319–3324.
(96) Parshall, G. W. *J. Am. Chem. Soc.* **1966**, *88*, 704.
(97) Parshall, G. W. *J. Am. Chem. Soc.* **1974**, *96* (8), 2360–2366.
(98) Ghosh, A. *J. Mol. Struct.* **1996**, *388*, 359–363.
(99) Anderson, H. L. *Chem. Commun.* **1999**, 2323–2330.
(100) Kashiwagi, Y.; Imahori, H.; Araki, Y.; Ito, O.; Yamada, K.; Sakata, Y.; Fukuzumi, S. *J. Phys. Chem. A* **2003**, *107*, 5515–5522.
(101) Suijkerbuijk, B. M. J. M.; Schamhart, D. J.; Kooijman, H.; Spek, A. L.; van Koten, G.; Klein Gebbink, R. J. M. Submitted for publication.

units, which gave the desired heteromultimetallic complexes $[M^1(M^2X(NCN))_4]$ in excellent yields. ^{195}Pt NMR spectroscopy convincingly showed the influence of the metal incorporated in the porphyrin core on the electron density at the Pt centers in the peripheral NCN-pincer complexes. UV/vis spectroscopic measurements furthermore established that the metallopincers influence the metalloporphyrin moiety.

Since we have found direct evidence for the possibility of fine-tuning the electron density of peripheral platinum centers by changing the *para*-metalloporphyrin substituent, we envisage that this effect is also exerted on the peripheral Pd centers. The use of this insight in the design of (ECE-pincer Pd)−porphyrin hybrids as tunable catalysts in C−C bond forming reactions is the subject of further investigations.[101,102]

Experimental Section

I. General. All air-sensitive reactions were performed under a nitrogen atmosphere with standard Schlenk techniques. All reactions involving porphyrin compounds were shielded from ambient light with aluminum foil. Et_2O and THF were carefully dried and distilled from sodium/benzophenone prior to use. CH_2Cl_2 and *N*,*N*-dimethylformamide (DMF) were distilled from CaH_2. Pyrrole was distilled from CaH_2 and stored at −30 °C. 3,5-Bis(hydroxymethyl)-4-bromoiodobenzene (**1**),[34] $[Zn(Br(NCN))_4]$,[51] $[Pd_2dba_3]\cdot CHCl_3$,[103] and $[Pt_2dipdba_3]$[43] were synthesized according to literature procedures. Column chromatography was performed with use of silica gel for column chromatography, 0.060−0.200 mm, pore diameter ca. 6 nm. ^{1}H and $^{13}C\{^1H\}$ NMR spectra were recorded at 300 and 75 MHz, respectively, at 298 K and were referenced to residual solvent signal. The ^{13}C NMR signals of the free-base porphyrin α- and *β*-carbon atoms were not resolved due to extreme line-broadening.[104] MALDI-TOF measurements were carried out with either 9-nitroanthracene (9NA) or 2,5-dihydroxybenzoic acid (DHB) as the matrix.

3,5-Bis(chloromethyl)-4-bromoiodobenzene (2). A mixture of 3,5-bis(hydroxymethyl)-4-bromoiodobenzene **1** (23.81 g, 69.42 mmol) and NEt_3 (24.4 mL, 174 mmol) in dry CH_2Cl_2 (350 mL) was cooled to 0 °C and subsequently treated with methanesulfonyl chloride (13.4 mL, 174 mmol) in a dropwise manner. At the end of the addition, all solids had dissolved to give a slightly yellow solution. This solution was allowed to warm to room temperature during which time a white precipitate formed. The suspension was then heated to reflux for 22 h, and allowed to cool to room temperature. Subsequently, H_2O (200 mL) was added to the resulting yellow solution, and stirring was continued for another 15 min. The layers were separated and the organic phase was washed with aqueous HCl (4 M, 200 mL) and brine (200 mL), dried ($MgSO_4$), and filtered. The filtrate was concentrated to dryness to leave an off-white solid. The solid was extracted with boiling hexane (6 mL/g) and the extract was evaporated to dryness. The resulting white fluffy solid was washed with cold hexanes (100 mL) and dried in vacuo. Yield: 24.40 g (93%). **Note: This compound is an extremely potent lachrymator and should be used immediately after its isolation!** ^{1}H NMR ($CDCl_3$) δ 7.78 (s, 2H, Ar*H*), 4.66 (s, 4H, CH_2Cl) ppm; GC-MS *m*/*z* 378 (60%, $[C_8H_6{}^{79}Br^{35}Cl_2I]^+$), 380 (100%, $[C_8H_6{}^{79}Br^{35}Cl^{37}ClI]^+ + [C_8H_6{}^{81}Br^{35}Cl_2I]^+$), 382 (40%, $[C_8H_6{}^{81}Br^{35}Cl^{37}ClI]^+$). Further characterization of this compound can be found in ref 35.

3,5-Bis(methoxymethyl)-4-bromoiodobenzene (3). A solution of sodium methoxide in methanol was prepared from sodium (3.39 g, 147 mmol) and MeOH (250 mL). Compound **2** (21.90 g, 57.66 mmol) was added to this clear solution at once and the resulting white suspension was stirred and heated. Just before the suspension reached reflux temperature, all solids had dissolved and after 5 min of continued stirring at reflux temperature a white microcrystalline solid began to precipitate (NaCl). After 4 h, the mixture was allowed to reach room temperature and all volatiles were subsequently evaporated. The remaining white residue was partitioned between Et_2O (200 mL) and H_2O (100 mL), the organic layer was isolated, and the aqueous layer was extracted with Et_2O (2 × 100 mL). The combined organic layers were dried ($MgSO_4$) and filtered, and the solvents were evaporated. The remaining white solid was recrystallized from hot methanol (7 mL/g) to yield white crystals, which were collected, washed with cold methanol, and dried in vacuo. Yield 19.20 g (90%). ^{1}H NMR ($CDCl_3$) δ 7.72 (s, 2H, Ar*H*), 4.47 (s, 4H, CH_2O), 3.48 (s, 6H, OCH_3) ppm; $^{13}C\{^1H\}$ NMR ($CDCl_3$) δ 140.1, 136.4, 122.1, 93.1, 73.5, 59.0 ppm; GC-MS *m*/*z* 370 (100%, $[C_{10}H_{12}{}^{79}BrIO_2]^+$), 372 (96%, $[C_{10}H_{12}{}^{81}BrIO_2]^+$). Anal. Calcd for $C_{10}H_{12}BrIO_2$: C 32.37, H 3.26. Found: C 32.46, H 3.23.

3,5-Bis(methoxymethyl)-4-bromobenzaldehyde (4). A white, turbid mixture of **3** (5.07 g, 13.7 mmol) in dry THF (200 mL) was treated dropwise with *t*-BuLi (18.2 mL, 1.5 M in pentane, 27.3 mmol) at −100 °C during 5 min. After 5 min of additional stirring at −100 °C, the resulting bright yellow solution was treated dropwise with dry DMF (2.8 mL, 36 mmol). After 5 min the light yellow suspension was allowed to reach room temperature. H_2O (10 mL) was subsequently added, which was followed by evaporation of all volatiles. Et_2O (150 mL) and H_2O (50 mL) were added, the mixture was vigorously stirred for 30 min, and the layers were separated. The water layer was extracted with Et_2O (2 × 50 mL) and the combined organic layers were washed with brine (300 mL), dried ($MgSO_4$), filtered, and concentrated to leave a yellow solid. Purification by column chromatography (Et_2O/hexanes 2:1, v/v) yielded **4** as a colorless crystalline material. Yield 3.26 g (86%). Further purification can be achieved by recrystallization at room temperature from hot hexanes (∼16 mL/g). ^{1}H NMR ($CDCl_3$) δ 10.02 (s, 1H, C*H*O), 7.91 (s, 2H, Ar*H*), 4.58 (s, 4H, CH_2O), 3.51 (s, 6H, OCH_3) ppm; $^{13}C\{^1H\}$ NMR ($CDCl_3$) δ 191.7, 139.6, 135.4, 128.9, 128.3, 73.8, 59.0 ppm; GC-MS *m*/*z* 272 (100%, $[C_{11}H_{13}{}^{79}BrO_3]^+$), 274 (98%, $[C_{11}H_{13}{}^{81}BrO_3]^+$). Anal. Calcd for $C_{11}H_{13}BrO_3$: C 48.37, H 4.80. Found: C 48.28, H 4.84.

5,10,15,20-Tetrakis[3,5-bis(methoxymethyl)-4-bromophenyl]-porphyrin (5). A refluxing, colorless solution of freshly prepared **4** (8.30 g, 30.4 mmol) in propionic acid (120 mL) was treated with freshly distilled pyrrole (2.12 mL, 30.4 mmol) and refluxing was continued for 40 min. The resulting black solution was stored at 6 °C overnight (refrigerator) and the resulting purple crystals were filtered off and washed with MeOH until the washings remained colorless. Yield 1.96 g (20%). ^{1}H NMR ($CDCl_3$) δ 8.83 (s, 8H, *β*-*H*), 8.25 (s, 8H, Ar*H*), 4.85 (s, 16H, CH_2O), 3.55 (s, 24H, OCH_3), −2.84 (s, 2H, N*H*) ppm; $^{13}C\{^1H\}$ NMR ($CDCl_3$) δ 141.4, 136.5, 133.9, 123.1, 119.2, 74.5, 59.0 ppm; UV/vis [λ_{max} (rel intensity), CH_2Cl_2] 420 (1.000), 516 (0.038), 552 (0.017), 592 (0.011), 647 (0.008) nm; ESI-HRMS *m*/*z* 1279.1068 ($[M + H]^+$), calcd for $C_{60}H_{59}Br_4N_4O_8$ 1279.1066. Anal. Calcd for $C_{60}H_{58}Br_4N_4O_8$: C 56.18, H 4.56, N 4.37. Found: C 56.24, H 4.45, N 4.31.

5,10,15,20-Tetrakis[3,5-bis(bromomethyl)-4-bromophenyl]-porphyrin (6). A red solution of **5** (0.98 g, 764 μmol) in CH_2Cl_2 (200 mL) was treated with HBr/HOAc (FRESH! 300 mL),

(102) Suijkerbuijk, B. M. J. M.; Herreras Mártinez, S. D.; van Koten, G.; Klein Gebbink, R. J. M. *Organometallics* **2008**, *27*, 534–542.
(103) Komiya, S. *Synthesis of Organometallic Compounds*; Wiley: New York, 1997.
(104) Shaw, S. J.; Shanmugathasan, S.; Clarke, O. J.; Boyle, R. W.; Osborne, A. G.; Edwards, C. E. *J. Porphyrins Phthalocyanines* **2001**, *5*, 575–581.

yielding a green solution, which was stirred at room temperature for 5 h. The resulting green suspension was cooled to 0 °C with use of an ice/water bath and ice water (500 mL) was added. After 5 min of vigorous stirring the layers were separated and the water layer was extracted once with CH_2Cl_2 (100 mL). The combined organic layers were vigorously stirred with 6 M K_2CO_3 solution in H_2O (500 mL) until the whole mixture attained a purple color and all solids had dissolved (due to the low solubility of $[\mathbf{6}(H^+)_2]^{2+}$ in H_2O and CH_2Cl_2 this can take approximately 2 h). The layers were again separated and the organic layer was dried ($MgSO_4$), filtered, and concentrated to 40 mL. Further purification with column chromatography (CH_2Cl_2/hexane 1:1, v/v), collection of the first purple band, and evaporation of the solvent yielded crude **6** as a purple solid. Yield 1050 mg (82%). The remaining chlorine contamination of this product can be oxidized to the corresponding porphyrin: the product was dissolved in CH_2Cl_2 (50 mL), DDQ (0.96 g, 4.23 mmol) was added, and the orange mixture was stirred for 2 h at room temperature. The mixture was filtered through a short pad of silica gel (CH_2Cl_2/hexane 4:1, v/v), which gave the title porphyrin as a purple, crystalline solid. ^{1}H NMR ($CDCl_3$) δ 8.91 (s, 8H, β-*H*), 8.28 (s, 8H, Ar*H*), 4.93 (s, 16H, CH_2Br), −2.90 (s, 2H, N*H*) ppm; $^{13}C\{^1H\}$ NMR ($CDCl_3$) δ 141.8, 137.4, 136.9, 126.8, 118.1, 33.9 ppm; UV/vis [λ_{max} (rel intensity), CH_2Cl_2] 422 (1.000), 517 (0.046), 551 (0.021), 591 (0.016), 648 (0.013) nm; MALDI-TOF MS (DHB) *m*/*z* 1674.44 ([M + H]$^+$), calcd for $C_{52}H_{35}Br_{12}N_4$ 1674.72. Anal. Calcd for $C_{52}H_{34}Br_{12}N_4$: C 37.32, H 2.05, N 3.35. Found: C 37.39, H 1.98, N 3.31.

5,10,15,20-Tetrakis(3,5-bis[(dimethylamino)methyl]-4-bromophenyl)porphyrin ([2H(Br(NCN))$_4$]). Porphyrin **6** (500 mg, 299 μmol) was dissolved in dry CH_2Cl_2 (100 mL) under a nitrogen atmosphere. The solution was treated with Me_2NH (1.0 mL, excess), and the resulting clear solution was stirred for 90 min. Degassed H_2O (60 mL) was added while stirring and after 30 min the two layers were separated. The organic layer was again washed with degassed H_2O (100 mL), dried ($MgSO_4$), filtered, and concentrated to 10 mL. Hexane (60 mL) was added and the purple solution was concentrated to 20 mL, whereupon crystallization of the product started to set in. The mixture was stored overnight at −30 °C, the supernatant was decanted, and the resulting purple, glistening crystals were dried in vacuo and stored under a nitrogen atmosphere. Yield 412 mg (99%). ^{1}H NMR ($CDCl_3$) δ 8.84 (s, 8H, β-*H*), 8.19 (s, 8H, Ar*H*), 3.85 (s, 16H, CH_2N), 2.43 (s, 48H, N(CH_3)$_2$), −2.81 (s, 2H, N*H*) ppm; $^{13}C\{^1H\}$ NMR ($CDCl_3$) δ 140.7, 137.3, 135.5, 127.3, 119.4, 64.4, 46.0 ppm; UV/vis [λ_{max} (rel intensity), CH_2Cl_2] 421 (1.000), 518 (0.038), 552 (0.020), 592 (0.011), 650 (0.010) nm; ESI-HRMS *m*/*z* 692.1800 ([M + 2H]$^{2+}$), calcd for $^1/_2C_{68}H_{84}Br_4N_{12}$ 692.1838. Anal. Calcd for $C_{68}H_{82}Br_4N_{12}\cdot C_6H_{14}$: C 60.33, H 6.57, N 11.41. Found: C 60.39, H 6.35, N 11.29.

[5,10,15,20-Tetrakis(3,5-bis[(dimethylamino)methyl]-4-bromophenyl)porphyrinato]nickel(II) ([Ni(Br(NCN))$_4$]). To a purple solution of [2H(Br(NCN))$_4$] (33.0 mg, 23.8 μmol) in dry toluene (10 mL) was added Ni(acac)$_2$ (122 mg, 476 μmol) and the resulting mixture was heated at reflux temperature for 3 h. After the reaction had completed (monitored by UV/vis spectroscopy) the volatiles were evaporated. The remaining red solid was partitioned between CH_2Cl_2 (10 mL) and water (10 mL) and the organic layer was isolated, dried ($MgSO_4$), and filtered. Hexane (20 mL) was added and the solution was concentrated to 10 mL and stored at −30 °C for 4 days. The resulting red/orange crystals were isolated by centrifugation. Yield 35 mg (100%). ^{1}H NMR ($CDCl_3$) δ 8.72 (s, 8H, β-*H*), 7.99 (s, 8H, Ar*H*), 3.78 (s, 16H, CH_2N), 2.38 (s, 48H, N(CH_3)$_2$) ppm; $^{13}C\{^1H\}$ NMR ($CDCl_3$) δ 142.9, 139.6, 137.5, 134.7, 132.1, 127.2, 118.4, 64.3, 45.9 ppm; UV/vis [λ_{max} (rel intensity), CH_2Cl_2]: 417 (1.000), 528 (0.090) nm; LDI-TOF MS *m*/*z* 1438.91 ([M]$^+$), calcd for $C_{68}H_{80}Br_4N_{12}Ni$ 1438.27. Anal. Calcd for $C_{68}H_{80}Br_4N_{12}Ni$: C 56.57, H 5.59, N 11.64, Ni 4.07. Found: C 56.50, H 5.68, N 11.51, 4.15. Crystals suitable for X-ray crystallographic analysis were obtained by slow evaporation of a saturated solution of [Ni(Br(NCN))$_4$] in hexane at room temperature.

Standard procedure for 4-fold palladation: A solution of [M^1(Br(NCN))$_4$] (M^1 = 2H, Ni, Zn) in dry benzene (2 mM) was treated with $[Pd_2dba_3]\cdot CHCl_3$ (4.5−4.8 equiv) and the solution was stirred for 16 h at room temperature under an N_2 atmosphere, yielding a turbid mixture. $HNEt_2$ (1 mL) was then added to decompose the unreacted $[Pd_2dba_3]\cdot CHCl_3$ and after 3 h of subsequent stirring at room temperature, all volatiles were removed in vacuo. The dark residue was dissolved in CH_2Cl_2 (5 mM) and the mixture was filtered over Celite into a centrifuge vessel and the Celite was washed with fresh CH_2Cl_2 until the washings were colorless (the Celite retains Pd^0). The volume of the filtrate was reduced to ∼10 mL and hexane (50 mL) was added, which resulted in (partial) precipitation of the product. The suspension was then concentrated to ∼20 mL and the now fully precipitated product was collected by centrifugation (10 min at 2400 rpm).

5,10,15,20-Tetrakis(3,5-bis[(dimethylamino)methyl]-4-bromidopalladio(II)phenyl)porphyrin ([2H(PdBr(NCN))$_4$]). Purple solid. Yield 90%. ^{1}H NMR ($CDCl_3$) δ 8.86 (s, 8H, β-*H*), 7.60 (s, 8H, Ar*H*), 4.27 (s, 16H, CH_2N), 3.16 (s, 48H, N(CH_3)$_2$), −2.79 (s, 2H, N*H*) ppm; $^{13}C\{^1H\}$ NMR ($CDCl_3$) δ 157.4, 143.5, 138.8, 131.1, 126.5, 120.6, 75.1, 53.7 ppm; UV/vis [λ_{max} (rel intensity), CH_2Cl_2] 426 (1.000), 522 (0.034), 558 (0.028), 594 (0.011), 653 (0.015) nm; MALDI-TOF MS (DHB) *m*/*z* 1811.04 ([M + H]$^+$), calcd for $C_{68}H_{83}Br_4N_{12}Pd_4$ 1811.99. Anal. Calcd for $C_{68}H_{82}Br_4N_{12}Pd_4$: C 45.05, H 4.56, N 9.27. Found: C 45.12, H 4.63, N 9.12.

[5,10,15,20-Tetrakis(3,5-bis[(dimethylamino)methyl]-4-bromidopalladio(II)phenyl)porphyrinato]nickel(II) ([Ni(PdBr(NCN))$_4$]). Orange solid. Yield 87%. ^{1}H NMR ($CDCl_3$) δ 8.76 (s, 8H, β-*H*), 7.39 (s, 8H, Ar*H*), 4.22 (s, 16H, CH_2N), 3.16 (s, 48H, N(CH_3)$_2$) ppm; UV/vis [λ_{max} (rel intensity), CH_2Cl_2] 423 (1.000), 531 (0.088) nm; MALDI-TOF MS (DHB) *m*/*z* 1789.73 ([M − Br]$^+$), calcd for $C_{68}H_{80}Br_3N_{12}NiPd_4$ 1788.98. Anal. Calcd for $C_{68}H_{80}Br_4N_{12}NiPd_4$: C 43.69, H 4.31, N 8.99, Ni 3.14. Found: C 43.84, H 4.38, N 8.78, Ni 3.30. The small quantity in which this compound was available did not allow for a satisfactory ^{13}C NMR measurement.

[5,10,15,20-Tetrakis(3,5-bis[(dimethylamino)methyl]-4-bromidopalladio(II)phenyl)porphyrinato]zinc(II) ([Zn(PdBr(NCN))$_4$]). Purple/greenish solid. Yield 90%. ^{1}H NMR ($CDCl_3$) δ 8.97 (s, 8H, β-*H*), 7.61 (s, 8H, Ar*H*), 4.27 (s, 16H, CH_2N), 3.17 (s, 48H, N(CH_3)$_2$) ppm; $^{13}C\{^1H\}$ NMR ($CDCl_3$) δ 156.5, 150.4, 143.2, 139.4, 132.0, 126.3, 121.4, 75.0, 53.7 ppm; UV/vis [λ_{max} (log ε), CH_2Cl_2] 429 (5.75), 554 (4.35), 596 (4.00) nm; ESI-MS *m*/*z* 1797.20 ([M − Br]$^+$), calcd for $C_{68}H_{80}Br_3N_{12}Pd_4Zn$ 1796.25. Anal. Calcd for $C_{68}H_{80}Br_4N_{12}Pd_4Zn$: C 43.53, H 4.30, N 8.96, Zn 3.49. Found: C 43.65, H 4.42, N 9.06, Zn 3.43. Crystals suitable for X-ray crystallographic analysis were obtained by slow evaporation of a solution of [Zn(PdBr(NCN))$_4$] (4 mg) in a mixture of CH_2Cl_2 and hexanes (2:1, v/v, 1.5 mL) and a drop of pyridine.

Standard procedure for 4-fold platination: A solution of [M^1(Br(NCN))$_4$] (M^1 = 2H, Ni, Zn) in dry benzene (1 mM) was treated with [Pt_2dipdba$_3$] (5 equiv) and the solution was stirred for 16 h at reflux temperature under an N_2 atmosphere, yielding a turbid mixture. $HNEt_2$ (1 mL) was then added to decompose the unreacted [Pt_2dipdba$_3$] and after 3 h of subsequent stirring at room temperature, all volatiles were removed in vacuo. The black residue was stirred in $CHCl_3$ (2 mM) with a saturated solution of NH_4Cl in H_2O for 48 h and the layers were separated. The organic layer was dried ($MgSO_4$) and filtered over Celite into a centrifuge vessel, and the Celite was washed with fresh CH_2Cl_2 until the washings were colorless (the Celite retains Pt^0). The volume of the filtrate was reduced to ∼10 mL

and hexane (50 mL) was added, which resulted in (partial) precipitation of the product. The suspension was then concentrated in vacuo to ~20 mL and the now fully precipitated product was collected by centrifugation (10 min at 2400 rpm).

5,10,15,20-Tetrakis(3,5-bis[(dimethylamino)methyl]-4-chloridoplatino(II)phenyl)porphyrin ([2H(PtCl(NCN))$_4$]). Purple microcrystalline solid. Yield 67%. ^{1}H NMR (CD_2Cl_2) δ 8.95 (s, 8H, β-*H*), 7.63 (s, 8H, Ar*H*), 4.31 (s, 16H, CH_2N), 3.27 (s, 48H, N(CH_3)$_2$), −2.77 (s, 2H, N*H*) ppm; ^{195}Pt NMR ($CDCl_3$) δ −3162 ppm; UV/vis [λ_{max} (rel intensity), CH_2Cl_2] 433 (1.000), 522 (0.058), 564 (0.056), 657 (0.026) nm; MALDI-TOF MS (DHB) *m*/*z* 1989.80 ([M + H]$^+$), calcd for $C_{68}H_{83}Cl_4N_{12}Pt_4$ 1989.41; *m*/*z* 1953.55 ([M − Cl]$^+$), calcd for $C_{68}H_{82}Cl_3N_{12}Pt_4$ 1953.44. Anal. Calcd for $C_{68}H_{82}Cl_4N_{12}Pt_4\cdot CHCl_3$: C 41.03, H 4.45, N 7.66. Found: C 40.54, H 4.10, N 7.56. A satisfactory ^{13}C{^{1}H} spectrum could not be recorded since the compound quickly crystallized from the solution.

[5,10,15,20-Tetrakis(3,5-bis[(dimethylamino)methyl]-4-chloridoplatino(II)phenyl)porphyrinato]nickel(II) ([Ni(PtCl(NCN))$_4$]). Orange solid. Yield 94%. ^{1}H NMR ($CDCl_3$) δ 8.80 (s, 8H, β-*H*), 7.40 (s, 8H, Ar*H*), 4.21 (s, 16H, CH_2N), 3.23 (s, 48H, N(CH_3)$_2$) ppm; ^{13}C{^{1}H} NMR ($CDCl_3$) δ 145.0, 142.8, 142.0, 136.1, 132.1, 125.2, 120.1, 78.0, 54.8 ppm; ^{195}Pt NMR ($CDCl_3$) δ −3170 ppm; UV/vis [λ_{max} (rel intensity), CH_2Cl_2] 431 (1.000), 534 (0.089) nm; MALDI-TOF MS (DHB) *m*/*z* 2011.79 ([M − Cl]$^+$), calcd for $C_{68}H_{80}Cl_3N_{12}NiPt_4$ 2012.36. Anal. Calcd for $C_{68}H_{80}Cl_4N_{12}NiPt_4$: C 39.91, H 3.94, N 8.21, Ni 2.87. Found: C 40.11, H 4.08, N 8.07, Ni 2.75.

[5,10,15,20-Tetrakis(3,5-bis[(dimethylamino)methyl]-4-chloridoplatino(II)phenyl)porphyrinato]zinc(II) ([Zn(PtCl(NCN))$_4$]). Purple/green microcrystalline solid. Yield 87%. ^{1}H NMR ($CDCl_3$) δ 9.01 (s, 8H, β-*H*), 7.63 (s, 8H, Ar*H*), 4.29 (s, 16H, CH_2N), 3.29 (s, 48H, N(CH_3)$_2$) ppm; ^{13}C{^{1}H} NMR ($CDCl_3$) δ 150.3, 144.7, 141.7, 138.1, 132.0, 126.0, 122.1, 78.1, 54.9 ppm; ^{195}Pt NMR ($CDCl_3$) δ −3176 ppm; UV/vis [λ_{max} (rel intensity), CH_2Cl_2] 435 (1.000), 555 (0.056), 599 (0.036) nm; MALDI-TOF MS (9NA) *m*/*z* 2017.70 ([M − Cl]$^+$), calcd for $C_{68}H_{80}Cl_3N_{12}ZnPt_4$ 2017.36. A completely satisfactory elemental analysis could not be obtained. Unfortunately, this compound was too immobile on either silica gel or alumina to allow for further purification by chromatographic means.

[5,10,15,20-Tetrakis(3,5-bis[(dimethylamino)methyl]-4-trichloridoplatino(IV)phenyl)porphyrinato]nickel(II) ([Ni(Pt(IV)Cl$_3$(NCN))$_4$]). A deep orange solution of ([Ni(PtCl(NCN))$_4$]) (14 mg, 6.8 μmol) in dry CH_2Cl_2 (5 mL) was treated with a solution of $CuCl_2\cdot 2H_2O$ (9.3 mg, 54.7 μmol) in EtOH (2 mL), which led to the immediate precipitation of a dark orange solid. After 30 min of continued stirring, the solid was filtered off, then washed with EtOH (5 mL), H_2O (2 × 10 mL), Et_2O (2 × 10 mL), and finally CH_2Cl_2 (2 × 10 mL) to give 15.9 mg of the title compound (quantitative yield). The solubility of this compound, even in hot DMSO, is so low that it precluded the recording of a satisfactory ^{1}H NMR spectrum. UV/vis [λ_{max} (rel intensity), CH_2Cl_2] 419 (1.000), 530 (0.083) nm. Anal. Calcd for $C_{68}H_{80}Cl_{12}N_{12}NiPt_4$: C 35.05, H 3.46, N 7.21, Ni 2.52. Found: C 35.18, H 3.60, N 7.17, Ni 2.50.

II. Complexation and Decomplexation of SO_2 to [M^1(PtCl(NCN))$_4$] (M^1 = 2H, Ni, Zn). Dry SO_2 gas was bubbled through a solution of the appropriate [M^1(PtCl(NCN))$_4$] in dry CH_2Cl_2 until no further changes in the absorption spectrum were noted. Decomplexation was accomplished by allowing the solution to stand open to air for at least 16 h, or alternatively by bubbling dry air through the solution of the SO_2 complex for at least 30 min.

III. Determination of Binding Constants. Solutions were prepared containing the zinc porphyrin of interest (~1 μM) and the appropriate amount of pyridine (200−1 000 000 equiv) in CH_2Cl_2. The absorbance of the resulting complex was monitored as a function of the concentration of pyridine. When {1/Δabsorbance} is then plotted against {1/[pyridine]}, the intercept with the X-axis is equal to −[binding constant].[105,106]

X-ray Crystal Structure Determinations. Reflections were measured on a Nonius Kappa CCD diffractometer with rotating anode (graphite monochromator, λ = 0.71073 Å) at a temperature of 150 K. Intensities were integrated with EvalCCD,[107] using an accurate description of the experimental setup for the prediction of the reflection contours. The structures were refined with SHELXL-97[108] against F^2 of all reflections. Non-hydrogen atoms were refined with anisotropic displacement parameters. Hydrogen atoms were introduced in calculated positions and refined with a riding model. Geometry calculations and checking for higher symmetry was performed with the PLATON program.[109]

Compound [Ni(Br(NCN))$_4$]: $C_{68}H_{80}Br_4N_{12}Ni$ + disordered solvent, Fw = 1443.79, red-orange block, 0.35 × 0.06 × 0.02 mm^3, monoclinic, *C*2/*c* (no. 15), *a* = 35.4380(10) Å, *b* = 9.8494(10) Å, *c* = 29.2457(10) Å, β = 126.113(1)°, *V* = 8246.6(9) Å^3, *Z* = 4, D_x = 1.163 g/cm^3 (derived parameters do not contain the contribution of the disordered solvent), μ = 2.21 mm^{-1} (derived parameters do not contain the contribution of the disordered solvent). A total of 77763 reflections were measured up to a resolution of (sin $\theta/\lambda)_{max}$ = 0.54 Å^{-1}. The reflections were corrected for absorption and scaled on the basis of multiple measured reflections with the program SADABS[110] (0.61−0.91 correction range). A total of 5378 reflections were unique (R_{int} = 0.1217). The structure was solved with the program SHELXS-86,[111] using Direct Methods. The crystal structure contains voids (2260 Å^3/unit cell) filled with disordered solvent molecules. Their contribution to the structure factors was secured by back-Fourier transformation, using the routine SQUEEZE of the program PLATON,[109] resulting in 551 electrons/unit cell. A total of 393 parameters were refined with 72 restraints. R1/*w*R2 [$I > 2\sigma(I)$]: 0.0647/0.1303. R1/*w*R2 [all reflections]: 0.1117/0.1463. *S* = 1.070. Residual electron density between −0.68 and 0.98 e/Å^3.

Compound {[Zn(PdBr(NCN))$_4$](pyridine)}: $C_{73}H_{85}Br_{1.84}Cl_{2.16}N_{13}Pd_4Zn\cdot 3C_7H_8\cdot 2CHCl_3$ + disordered $CHCl_3$, Fw = 2374.25 (derived parameters do not contain the contribution of the disordered solvent), purple block, 0.39 × 0.24 × 0.18 mm^3, triclinic, $P\bar{1}$ (no. 2), *a* = 15.126(3) Å, *b* = 19.255(4) Å, *c* = 20.943(5) Å, α = 111.226(3)°, β = 95.283(3)°, γ = 101.042(3)°, *V* = 5493(2) Å^3, *Z* = 2, D_x = 1.435 g/cm^3 (derived parameters do not contain the contribution of the disordered solvent), μ = 1.77 mm^{-1} (derived parameters do not contain the contribution of the disordered solvent). A total of 125122 reflections were measured up to a resolution of (sin $\theta/\lambda)_{max}$ = 0.65 Å^{-1}. The reflections were corrected for absorption and scaled on the basis of multiple measured reflections with the program SADABS[110] (0.61−0.73 correction range). A total of 25199 reflections were unique (R_{int} = 0.0329). The structure was solved with the program DIRDIF99,[112] using automated Patterson Methods. The crystal structure contains voids (824 Å^3/unit cell) filled with

(105) Benesi, H. A.; Hildebrand, J. H. *J. Am. Chem. Soc.* **1949**, *71*, 2703–2707.
(106) Schneider, H.-J.; Yatsimirsky, A. *Principles and Methods in Supramolecular Chemistry*; John Wiley & Sons: New York, 1999.
(107) Duisenberg, A. J. M.; Kroon-Batenburg, L. M. J.; Schreurs, A. M. M. *J. Appl. Crystallogr.* **2003**, *36*, 220–229.
(108) Sheldrick, G. M. *SHELXL-97*; University of Göttingen: Göttingen, Germany: 1997.
(109) Spek, A. L. *J. Appl. Crystallogr.* **2003**, *36*, 7–13.
(110) Sheldrick, G. M. *SADABS*; University of Göttingen: Göttingen, Germany: 1999.
(111) Sheldrick, G. M. *SHELXS-86*; University of Göttingen: Göttingen, Germany: 1986.
(112) Beurskens, P. T.; Admiraal, G.; Beurskens, G.; Bosman, W. P.; Garcia-Granda, S.; Gould, R. O.; Smits, J. M. M.; Smykalla, C. *DIRDIF99*; University of Nijmegen: Nijmegen, The Netherlands, 1999.

disordered $CHCl_3$ solvent molecules. Their contribution to the structure factors was secured by back-Fourier transformation, using the routine SQUEEZE of the program PLATON,[109] resulting in 190 electrons/unit cell. The halogenide position was refined with a partial occupation by chlorine (54%) and by bromine (46%) and the Pd−halogen distances were restrained, respectively. A total of 1129 parameters were refined with 175 restraints. R1/*w*R2 [$I > 2\sigma(I)$]: 0.0408/0.1150. R1/*w*R2 [all reflections]: 0.0619/0.1230. $S = 1.141$. Residual electron density between −1.42 and 1.55 e/Å^3.

Acknowledgment. The Dutch council for scientific research (NWO) is gratefully acknowledged for financial support (D.M.T., M.L., and A.L.S.) and for a "Jonge Chemici" scholarship (B.M.J.M.S. and R.J.M.K.G.).

Supporting Information Available: ^{1}H NMR and mass spectra of all reported compounds, $^{13}C\{^1H\}$ spectra of selected compounds, and crystallographic information files (CIF) for [**Ni**(**Br**(**NCN**))$_4$] and {[**Zn**(**PdBr**(**NCN**))$_4$](**pyridine**)}. This material is available free of charge via the Internet at http://pubs.acs.org.